ANALYSIS OF SIMPLE 2-D AND 3-D METAL STRUCTURES SUBJECTED TO FRAGMENT IMPACT*

E.A. Witmer, T.R. Stagliano, R.L. Spilker, and J.J.A. Rodal

Aeroelastic and Structures Research Laboratory
Department of Aeronautics and Astronautics
Massachusetts Institute of Technology

SUMMARY

Reviewed in this paper are studies carried out and/or in progress at the MIT Aeroelastic and Structures Research Laboratory to develop theoretical procedures for predicting the large-deflection elastic-plastic transient structural responses of metal containment or deflector structures to cope with rotor-burst fragment impact attack. Most of the past effort was devoted to containment/deflector (C/D) structures whose axial dimension is comparable to that of the attacking fragments and hence the associated structural responses are essentially two-dimensional. Recent effort has been applied to analyzing C/D structures whose "axial dimension" is much larger than that of the attacking fragments; thus, the associated structural response to be analyzed is essentially three-dimensional.

For two-dimensional C/D structures both finite-element and finite-difference analysis methods have been employed to analyze structural response produced by either (a) prescribed transient loads or (b) fragment impact. For the latter category, two time-wise step-by-step analysis procedures have been devised to predict the structural responses resulting from (a succession of) fragment impacts: (1) the collision force method (CFM) whereby one utilizes an approximate prediction of the force applied to the attacked structure during fragment impact (also equal and oppositely to the fragment itself) and (2) the collision imparted velocity method (CIVM) in which one computes the impact-induced velocity increment acquired by a region of the impacted structure near the impact point (and the attendant velocity decrement suffered by the attacking fragment). The merits and limitations of these approaches are discussed. For the analysis of 3-d responses of C/D structures, only the CIVM approach is being investigated.

Experimental data for assessing the accuracy, limitations, and versatility of these analyses have been obtained from two sources. The Naval Air Propulsion Test Center has provided data on the responses of containment rings to (a) a single T58 turbine rotor blade and (b) to tri-hub burst fragment attack from a T58 turbine rotor. Simpler impact experiments involving a "non-deformable fragment" (a solid steel sphere) against simple aluminum beams and panels have been conducted at the MIT Aeroelastic and Structures Research Laboratory. Comparisons of predictions with observed structural response data are discussed.

* This research has been supported in large part by the NASA Lewis Research Center under NGR 22-009-339; the authors wish to acknowledge also the help of their various colleagues (see co-authors cited in references of Appendices A and B).

1. Introduction

Engine rotor burst fragments may impact against the engine casing and/or against special protective structures. These structures may be intended either to contain or to divert the fragment and to allow it to escape along a "harmless" path; the respective behavior is termed as being either fragment containment or fragment deflection. Of principal interest in this paper is the theoretical prediction of container or deflector structures (C/D structures) which are subjected to fragment impact. Further, attention is restricted to single-layer metallic protective structures; the use of non-metallic materials for protective structures undergoing fragment impact is addressed by several other papers in this Workshop.

If the dimension of the protective structure in the direction parallel to the axis of rotation of the turbojet engine is comparable to the corresponding dimension of the attacking fragment, the deflection of the attacked structure will be essentially the same at all locations along that axial direction; in this case, the deformation is termed two-dimensional (2-D). However, if that protective-structure dimension is large in the above comparative sense, the structure will undergo general three-dimensional (3-D) structural deflections.

For preliminary design and parametric studies of C/D structures, it may be useful to idealize the transient structural response as 2-D, as depicted schematically in Fig. 1. Here the effect of the structure which supports the C and/or D structure is represented by a normal and tangential spring foundation; also, various support conditions can be provided in this type of idealized 2-D model. This type of model tends to include the main structural response features while minimizing the computational burden. Accordingly, a series of 2-D structural response codes for partial and/or complete rings of arbitrary initial shape, with uniform or nonuniform thickness, and subjected to initial-velocity distributions, prescribed externally-applied loads, or fragment impact have been developed. The capabilities and features of these computer codes [1-5]* are summarized in Appendix A. Some illustrative examples of the use of some of these codes are shown later in this paper.

For structural response conditions wherein the use of a 2-D idealization is an excessive over-simplification and where one seeks to predict the response in greater detail, the structure needs to be modeled as an assemblage of shell elements (and stiffeners) [6-8] to enable an accounting of the 3-D shell

*References are indicated by numbers in square [ ] brackets.

structural deflections which are present. On the other hand an excessively fine modeling such as the use of 3-D solid elements to represent a single-layer shell, stiffeners, etc. leads to an excessive computational burden for many purposes. Hence, "shell behavior" modeling serves as a logical "next improvement" over 2-D modeling of C/D structures. Accordingly, theoretical prediction methods to compute the responses of plates and shells to initial velocity distributions and prescribed externally-applied transient loads [6] are being adapted to predict structural response to fragment impact [9].

In order to evaluate the accuracy and adequacy of these structural response prediction methods, various experiments have been carried out. The Naval Air Propulsion Test Center (NAPTC) has provdied data on the responses of aluminum and steel containment rings to (1) impact by a single T58 turbine rotor blade and (2) to tri-hub burst fragment attack from a T58 turbine rotor ([10-13], for example); in these cases the attacking fragment is complex and undergoes a considerable amount of deformation during its impact interaction with the containment ring. A cleaner, less-complex set of impact experiments has been conducted at the MIT Aeroelastic and Structures Research Laboratory, involving steel-sphere impact against (1) beams, (2) uniform-thickness initially-flat square aluminum panels, and (3) panels of type (2) but with integral stiffeners of rectangular cross section; transient strain, permanent strain, and permanent deflection data of good reliability and accuracy for comparison with predictions were obtained [14,15]. Some of these studies are described briefly in the following.

At the present time, theoretical-experimental correlation studies utilizing the NAPTC and the MIT-ASRL experimental data are in progress for the 2-D cases; for these cases the CIVM-JET 4B computer code is being employed. For fragment-impact panels (which undergo 3-D responses), some preliminary calculations are under way using the breadboard CIVM-PLATE code; systematic testing and checking of this code will be required before it can be used with confidence.

Figure 2 serves as a concise outline of most of the MIT-ASRL studies which have been carried out to date concerning the theoretical prediction of the responses of metallic C/D structures to fragment impact. Listed in Appendix B are the associated MIT-ASRL reports and papers, as well as the status and availability of the pertinent structural response computer codes.

Section 2 is devoted to describing two of the analysis methods (the collision imparted velocity method CIVM, and the collision force method CFM) studied for predicting the large-deflection, elastic-plastic, transient responses of 2-D structures which are subjected either to impulse loading or to fragment impact attack; illustrative examples of the application of these methods are shown, with emphasis on the CIVM approach. Section 3 deals with theoretical and experimental studies of fragment-impact-induced responses of panels which undergo 3-D structural responses. Comments are given in Section 4 concerning the status of structural response prediction procedures for 2-D and 3-D single-layer metallic C/D structures, as well as observations concerning analysis needs for multilayer multimaterial C/D concepts and configurations being considered as lighter weight candidates to cope with energetic engine rotor burst fragments.

2. 2-D Structural Response Studies

Some representative analyses and results will be illustrated here concisely; more extensive results and discussion may be found in the cited references. Analysis of 2-D structural response to fragment impact will be discussed for two approaches: the collision imparted velocity method (CIVM) and the collision force method (CFM); for illustration, both approaches are applied to analyze the transient response of a containment ring to impact by a single blade of a turbine rotor. Next, a more complex fragment attack is analyzed by using the CIVM approach; this involves T58 tri-hub turbine rotor burst attack against a steel containment ring. Because of the complexities arising mainly from severe changes in the geometries of the attacking fragments during the impact and interaction process, it became advisable to obtain experimental data for a more clearly defined impact situation in order that the measured transient response information could be used to make a clear assessment of the adequacy of the basic building blocks contained in the theoretical prediction procedure. Accordingly, described next are experimental and theoretical studies of the transient responses of simple beams to impulse loading or to steel sphere impact attack.

2.1 Single Rotor Blade Impact Against a Containment Ring

In these studies of 2-D structural response to impact, use is made of finite element and finite difference methods which have been shown to produce

reliable predictions for large-deflection, elastic-plastic, transient response of simple beams and rings subjected to known impulsive loading [16,17]. For impact-induced structural response analysis, the principal added ingredient to be taken into account is the impact/interaction itself; two methods (CIVM and CFM) explored for treating this matter are discussed next.

To illustrate these approaches, impact of a single blade from a T58 turbine rotor against a containment ring will be studied. High speed photographic data for such a case have been obtained at the spin-chamber facility of the Naval Air Propulsion Test Center [10]. Ring configuration data and blade orientation as a function of time at intervals about 30 microseconds apart were obtained and are used for illustrative comparisons.

2.1.1 Analysis with the Collision Imparted Velocity Method

Figure 3 illustrates a containment ring which is modeled by a number of finite elements and subjected to impact attack by an idealized single rotor blade. The equations of motion for the ring and for the fragment are solved in small increments Δt in time by an appropriate finite-difference time operator scheme. For this analysis, the fragment is regarded as being rigid. Impact is regarded as being an instantaneous local effect between the fragment and a small region of the structure in the vicinity of the impact point; for present purposes, the size of this small ring region on either side of the impact point is estimated as being the product of Δt and the longitudinal elastic wave speed in the ring. Impulse/momentum and kinetic energy conservation equations are used to calculate the "post-impact" (or collision-imparted) velocities of the fragment and of this impact-affected structural region; by employing the concept of the coefficient of restitution (e) this local impact can be treated as perfectly elastic (e=1), perfectly inelastic (e=0), or intermediate ($0<e<1$).

Figure 4 is an information flow diagram illustrating the use of this "collision-imparted velocity method" (CIVM) in the calculation of transient structural response produced by fragment impact. Typically, a succession of impacts is predicted. Fuller details of this approach are given, for example, in Refs. 4, 17, and 18.

Table 1 summarizes the containment ring and fragment data for the illustrative case: NAPTC Test 91. Shown in Fig. 5 are predicted and measured deformed ring configurations and blade locations at 150, 570, and 810 microseconds after initial impact. In the impact quadrant the ring was modeled by 10 equal length

cubic-cubic elements; 6 equal-length elements were used in each of the 3 other quadrants. For these calculations, coefficients of restitution of e=0 and e=1 were used. The 6061-T6 aluminum ring material was regarded as elastic, perfectly-plastic, with a strain-rate (EL-PP-SR) dependent yield stress σ_y given by the following approximation:

$$\sigma_y = \sigma_o[1 + |\frac{\dot{\varepsilon}}{D}|^{\frac{1}{p}}]$$

where σ_o is the static yield stress, $\dot{\varepsilon}$ is the strain rate, and D and p are material constants. For these calculations, D=6500 sec^{-1} and p=4 were assumed. Also, frictionless impact and interaction (μ=0) between the ring and the blade was assumed for the cases illustrated here. Fairly good agreement between the predicted and observed deformed ring configuration is noted, but the predicted vs. observed fragment motion is not good. This latter disagreement stems mainly from ignoring friction and the changing mass moment of inertia of the actual deforming blade. Later calculations included these effects.

2.1.2 Analysis with the Collision Force Method

In this method the attacking fragment is treated as being deformable. Shown, for example, in Fig. 6 are some postulated idealized configurations to represent a deformable impacting blade. The straight rigid blade model was used in the previous case. Explored in Ref. 19 were the following two idealizations -- the blade was assumed (a) to remain straight but to shorten in an elastic, perfectly-plastic (EL-PP) fashion or (b) to curl in a simple plausible assumed-mode fashion; these are termed, respectively, the elastic, perfectly-plastic shortening blade model (EL-PP-SB) and the elastic, perfectly-plastic curling blade model (EL-PP-CB). These modes of behavior combined with a step by step collision inspection set of rules permitted following this process. At any given instant, applicable values of governing geometric deformed-blade-configuration parameters were identified. These in turn were related via energy methods to the component of the force applied by the blade perpendicular to the surface of the attacked containment ring and equal-and-oppositely to the fragment itself. Similarly, equal and opposite tangential forces (from friction) were postulated to be μ times the normal-to-the-surface component. A self-explanatory information flow chart for the CFM process is given as Fig. 7.

Shown in Fig. 8 are defomed ring predictions at two instants after initial

impact for the EL-PP-SB model and the EL-PP-CB model for the case in which the friction coefficient μ is assumed to be .15 and the perfectly-plastic yield stress of the steel-alloy blade is assumed to be σ_{y_f} = 160,000 psi. Fairly good agreement between experiment and these EL-PP-CB model predictions is observed. Reference 19 shows the ring response to be rather insensitive to (plausible) values of friction coefficient used. The motion of the blade, however, is much more sensitive to μ -- as Fig. 9 indicates.

The curling blade model [19] devised by plausible engineering rules and approximations appears to represent rather well the behavior and the observed deformed configuration of the actual single blade in NAPTC Test 91. One must keep track of the time-varying geometry of both the deforming blade and the deforming containment ring in order to determine when and where the successive collisions (i.e., attempted simultaneous occupancy of some regions of space) occur. Hence, it is evident that if one were to use this method to analyze structural response to impact by, for example, a disk-rim fragment with perhaps 3 to 10 attached blades (each of which will undergo sequential different deformations), one would be faced with a substantial book-keeping job to define the space occupancy of this complex deforming fragment; the advisability of seeking a less complex scheme is clear. Accordingly, subsequent attention has been given to the use of greatly-idealized rigid fragments in conjunction with the CIVM analysis scheme.

2.2 CIVM Analysis of Tri-Hub Rotor Burst Attack Against a Containment Ring

One type of postulated engine rotor fragment attack which has received much discussion is that in which the rotor bursts into 3 equal segments (termed a tri-hub burst). One fragment of this type is shown schematically in Fig. 10. The NAPTC has conducted many tests involving tri-hub burst attack against various single-layer and multilayer containment rings. Recently NAPTC Test 201 involving tri-hub burst attack of a T58 turbine rotor at 19,859 rpm against a cast 4130 steel containment ring of 7.50-in inner radius, 0.625-in thickness, and 1.50-in axial length was conducted [13]. Figure 11 shows the post-test deformed-ring configuration. High speed photographs showed the severe deformation incurred by many of the blades during the impact/interaction process; this is depicted schematically in Fig. 10.

For convenience and geometric simplicity, each such fragment has been idealized for use in the CIVM-JET 4B computer code [4] as a rigid circular body

of the same mass and mass moment of inertia as the pre-impact fragment, with the same CG location, translational velocity, and rotational velocity as the actual fragment at postulated release. As indicated in Fig. 10, one might elect to represent the actual fragment by an idealized fragment of "properly selected radius r_f". An examination of this rotor indicates that reasonable minimum and maximum values for r_f would be about 2.56 and 4.20 inches, respectively; the use of these as well as an "intermediate" value of 3.36 inches was explored.

Figure 12 indicates the geometric, test, and modeling data for this case. The ring has been modeled by 48 equal-length ring elements. The point of initial impact of each of the three fragments is indicated in Fig. 12; element numbers and node identification are also given. The uniaxial static stress-strain properties of 4130 cast steel were approximated by piecewise linear segments with the stress-strain pairs: (σ,ε) = 80,950 psi, .00279; 105,300 psi, .0225; and 121,000 psi, .200 via the mechanical sublayer model; strain rate effects were approximated by using D = 40.4 sec^{-1} and p=5. Shown in Fig. 13 is the predicted ring configuration at 1000 microseconds after initial impact. The predicted inner surface and outer surface strains at the midelement location of elements 1, 4, and 6 are given in Fig. 14; for this calculation, frictionless impact μ=0 and r_f=2.555-in were employed. Figure 15 shows the circumferential distributions of inner-surface and outer-surface strain at 2400 microseconds after initial impact.

The effects of friction for otherwise identical modeling are indicated roughly by the Fig. 16 comparison of deformed ring configurations at 1200 microseconds after initial impact for μ=0 and μ=0.3. Similarly, the effects of idealized fragment radius r_f are seen in Fig. 16 where deformed ring profiles at 1200 microseconds after initial impact are shown for r_f=2.555-in and r_f=3.360-in. It is evident that if one chooses an unduly large idealized fragment radius r_f, this "rigid fragment" will constrain the ring to restrict its bending strain contribution so that unrealistically small total strains will be produced at the "convex lobes" -- compared with that which the actual "effectively-smaller-radius" fragment will produce.

The use of an idealized fragment of constant radius will clearly make it impossible to obtain complete time history agreement between predicted and measured inner-surface and/or outer-surface strains. However, the hope is that a properly-chosen effective r_f will lead to reasonable predictions vs. experiment

of maximum strains produced as a function of circumferential location. Further calculations and measurements are needed to assess the reliability with which this can be done. However, at the cost of greater complexity and computational expense, one can devise and use a fragment model which more closely simulates the behavior of the actual fragment.

Note, finally, that a comparison between the predicted and observed permanently-deformed ring configuration is not shown. This is the case because the calculation at Δt=1 microsecond has been carried out only to 2400 microseconds after initial impact. Whereas peak response occurred near 1200 microseconds, the ring is still springing back considerably at the 2400 microsecond time. A longer calculation would be necessary in order to permit making a reasonable estimate of the permanent-deformation configuration.

2.3 Beam Response to Steel Sphere Impact

In order to obtain appropriate and detailed 2-D transient structural response data under well-defined impact conditions so that a definitive evaluation could be made of the adequacy of the approximate collision-interaction analysis employed in the CIVM scheme, some simple experiments have been conducted at the MIT-ASRL. Beams of 6061-T651 aluminum with nominal 8-in span, 1.5-in width, and 0.10-in thickness and with both ends ideally clamped (see Fig. 18) have each been subjected to midspan impact by a solid steel sphere of one-inch diameter [14]. Impact velocities ranged from those sufficient to produce small permanent deflection to those needed for threshold rupture of the beam. Spanwise-oriented strain gages were applied to both the upper and the lower (impacted) surface of the beam at various spanwise locations. In each test, transient strain measurements were attempted for 8 of the gages; after each test, permanent strain readings were obtained for all surviving gages. Also, permanent deflection measurements were made.

An inspection of each specimen indicates that except near the point of impact itself (i.e., where $|x| \gtrsim 0.8$-in), the beam underwent essentially 2-D deflection behavior; pronounced 3-D behavior occurs near the point of initial impact. Hence, the 2-D structural response code (CIVM-JET 4B) may be expected to provide valid comparisons for $|x| \gtrsim 0.8$-in. Accordingly, such calculations and comparisons are in progress, and some preliminary results are shown next.

For the test and specimen identified as CB-18 in Ref. 14, the entire beam has been modeled with 43 equal-length cubic-cubic finite elements. The beam

material has been modeled as having either elastic, strain-hardening (EL-SH) or EL-SH-SR behavior where the uniaxial static stress-strain curve has been approximated by the σ,ε pairs: σ,ε= 41,000 psi, .0041; 45,000 psi, .0012; and 53,000 psi, .1000. For EL-SH-SR conditions, D=6500 sec^{-1} and p=4 have been assumed. For CB-18 initial steel-sphere impact occurred at a velocity of 2974 in/sec; a state of large permanent deflection was produced.

Shown in Fig. 19 are predicted and measured strains at spanwise stations x=1.50 and 1.20-in from the midspan impact point. At these 2-D structural response locations, there is fairly reasonable agreement between predicted and measured strains. Figure 20 shows the predicted transient vertical displacement response at x=1.0-in for both the EL-SH and the EL-SH-SR case. From these and longer-duration plots, the estimated respective permanent deflection is 0.63 and 0.58-in; the measured value is 0.60-in. While the comparisons shown here indicate encouraging agreement, more extensive calculations and comparisons are needed before a firm assessment can be made of the adequacy of the procedure embodied in the CIVM-JET 4B computer code [4].

3. 3-D Structural Response Studies

Of concern here are situations in which the fragment-impacted structure undergoes pronounced 3-D rather than 2-D deformation. Appropriate methods of structural response analysis and corresponding well-defined experimental transient structural response data which will serve to permit making a clear evaluation of the adequacy and/or accuracy of proposed prediction schemes are needed. Some contributions to this process are described here.

Although structural response analyses for fragment impact against initially-curved as well as initially-flat target structures are of interest, it is useful to minimize the complexities while checking the adequacy of the basic building blocks in the analysis process. Hence, attention has centered on impulse and impact experiments and theoretical analysis of initially-flat structures. Experiments involving steel-sphere impact against (1) narrow-plate (or beam) specimens [14] as well as (2) square uniform-thickness panels with four clamped edges and (3) panels of type (2) but with integrally-machined stiffeners of rectangular cross-section [15] have been conducted.

Two of the type (2) initially-flat specimens have been subjected to well-defined impulse loading by the sheet explosive loading technique to produce large-deflection, elastic-plastic transient structural response data for checking

the basic finite-element and transient response prediction aspects -- independent of impact itself. Also, steel sphere impact tests of this type of panel have been conducted. Thus, transient strain, permanent strain, and permanent deformation data of high quality are available for checking the prediction procedures of Refs. 6 and 9; the latter pertains to the breadboard computer codes PLATE and CIVM-PLATE which hopefully will enable one to predict 3-D transient large-deflection elastic-plastic, structural responses of panels caused by impulse and impact, respectively. If future correlation calculations reveal these codes to provide reliable transient response predictions, these codes will be upgraded to a condition convenient for routine use.

To illustrate the general character of the panel deformations produced for this purpose, Fig. 21 shows the permanent deflection along the centerline of specimen CP-2, a 0.062-in thick square initially-flat 8-in by 8-in panel of 6061-T651 aluminum with all four edges ideally clamped. The sheet explosive loading technique was used to impart essentially a uniform initial normal velocity of 16,235 in/sec over a 2-in by 2-in region centered at the panel center. Strain gages were also applied at various locations on the non-loaded side of the panel; both transient and permanent strain data were recorded. In addition, a pattern of lightly scribed grids was applied to a 3-in by 3-in region centered at the panel center on the non-loaded surface. Measurements of pre-test and post-test spacings of these grid lines enable one to make a rough determination of the permanent relative elongation on that surface as a function of location from the center of the panel. Some results from these determinations are shown in Fig. 22.

Steel sphere impact against a square 8-in initially-flat 6061-T651 aluminum panel of 0.063-in thickness with all four sides ideally clamped results in permanent deformation conditions wherein severe permanent deformation is concentrated near the point of initial impact itself as Fig. 23 shows for panel specimens CP-8 which suffered 1-inch diameter steel-sphere impact at 2435 in/sec. Photo-etched grids spaced 0.020-in apart on the non-impacted surface permitted making the permanent relative elongation measurements indicated in Fig. 24; the "large strains" are seen to be concentrated near the impact location and decrease rapidly with distance from the center of impact.

Finally, some illustrative preliminary results from applying the breadboard CIVM-PLATE code to steel-sphere-impacted narrow-plate (or beam) specimen

CB-18 are presented here; the steel-sphere impact velocity was 2794 in/sec initially. For computational thrift, one quarter of the specimen (see Fig. 18) was modeled by a 2 by 11 mesh of flat plate elements having 6 degrees of freedom per node, with symmetry conditions imposed along x=0 and y=0; this finite element mesh is shown in Fig. 25. Initial impact was assumed to occur at (x,y)=(0,0) whereas it actually occurred at about .06-in from this location. Relative elongation time histories predicted in this calculation along y=0 at stations x=0.6-in and x=1.2-in are compared with experimental measurements in Fig. 26. Figure 27 demonstrates that this 3-D structural response model exhibits 3-D deflection predictions -- vertical displacements predicted along y=0 (the centerline), y=.375-in, and y=.75-in as a function of spanwise location x are shown at 800 microseconds after initial impact. The anticipated larger displacement is seen to occur along y=0, with decreasing displacements (at given x-locations) more remote from the center of impact. Finally, Fig. 28 shows the predicted lateral transient deflection of the center of the plate (x,y)=(0,0) and the observed permanent deflection at this location; reasonable agreement is evident.

4. Summary Comments

Presented here is an overview of some of the work carried out to develop simple methods for predicting the 2-D transient large-deflection elastic-plastic structural responses of metal containment or deflection structures subjected to impulse loads or fragment impact; many more details may be found in the cited references. This 2-D type of idealization may serve as a good representation of certain fragment/structure impact/interaction situations or as a reasonable first approximation to other more complex cases. This 2-D idealization is relatively inexpensive to apply and may be useful for preliminary design, parametric studies, materials screening, etc. Structural configurations of 2-D type included in this discussion consist of complete rings, partial rings, constant or variable thickness, and uniform or arbitrarily-varying initial curvature, with various elastic foundation or various local support conditions provided. The associated computer codes (see Appendices A and B) are:

Structure Subjected to Prescribed Transient Loads or Initial Velocity Distributions

JET 3: Single-Layer Structures

JET 5A: Multilayer Bernoulli-Euler Structures

Structure Subjected Only to Fragment Impact

CIVM-JET 4B: Single-Layer Structures

CIVM-JET 5B: Multilayer Bernoulli-Euler Structures

Comparisons between experiment and predictions indicate good theoretical-experimental agreement for JET 3 predictions and a very encouraging but incomplete assessment for CIVM-JET 4B; further assessment studies are in progress.

For cases in which the impulsively-loaded structure [6] or fragment-impacted structure [9] undergoes significant 3-D structural responses, this more complex behavior must be modeled accordingly. Excellent theoretical-experimental agreement has been demonstrated [6] for finite-element analysis of plates and curved shells which undergo large-deflection elastic-plastic deformations in response to known severe impulse loading. Shown in this paper are encouraging preliminary comparisons between theory and experiment for fragment-impacted structures exhibiting 3-D structural response. Appropriate high quality experimental data on steel-sphere-impacted narrow beams, square uniform thickness panels, and longeron-stiffened initially-flat panels are available for near-future theoretical-experimental correlation studies to assess the accuracy and/or adequacy of the proposed prediction procedures. These studies are expected to suggest useful prediction modifications and improvements. Extensions to include fragment-impacted initially-curved 3-D structures would comprise a useful logical addition to the prediction capability.

Although this discussion has pertained to initially-isotropic metallic protective structures, many but not all of these analysis features can be carried over to the analysis of multilayer multimaterial protective structures -- such configurations are of potential future interest, as other papers in this Workshop indicate. Although such configurations will be much more complex and difficult to analyze, a validated structural response analysis capability would be of considerable value for preliminary design, materials screening, parametric studies, and to reduce the amount of ad hoc testing which otherwise would be required. The development and checking of accurate prediction methods to accommodate structural configurations and materials such as those cited at this Workshop in the presentations, for example, of Gerstle, Gardner, and Holms will be a difficult and lengthy process but will represent a highly useful state-of-the-art advance. This development and validation will require making

careful and detailed transient response observations and measurements for well-defined targets (geometry, boundary conditions, material mechanical and failure properties) and impact conditions. Realistic types of rotor-burst fragments should be used in exploratory experiments and in evaluation experiments; such experiments are essential to reveal the principal phenomena and to insure that important response features are not overlooked -- as might be the case if only highly simplified impact experiments were to be conducted. However, simpler better-defined fragments should be used to minimize uncertainties when obtaining detailed transient response data which are intended to serve as a definitive test of the accuracy and/or adequacy of the key building blocks of the procedures proposed for predicting the "threshold containment levels" of structural responses of multilayer multimaterial C/D structures.

REFERENCES

1. McCallum, R.B., Leech, J.W. and Witmer, E.A., "Progress in the Analysis of Jet Engine Burst-Rotor Containment Devices", ASRL TR 154-1, Aeroelastic and Structures Research Laboratory, Massachusetts Institute of Technology, August 1969. (Available as NASA CR-107900.)

2. McCallum, R.B., "Simplified Analysis of Trifragment Rotor Dist Interaction with a Containment Ring", AIAA Journal of Aircraft, Vol. 7, No. 3, May-June 1970, pp. 283-285.

3. Wu, R.W.-H. and Witmer, E.A., "Computer Program - JET 3 - to Calculate the Large Elastic-Plastic Dynamically-Induced Deformations of Free and Restrained, Partial and/or Complete Structural Rings", ASRL TR 154-7, Aeroelastic and Structures Research Laboratory, Massachusetts Institute of Technology, August 1972. (Available as NASA CR-120993.)

4. Stagliano, T.R., Spilker, R.L. and Witmer, E.A., "User's Guide to Computer Program CIVM-JET 4B to Calculate Large Nonlinear Transient Deformations of Single-Layer Partial and/or Complete Structural Rings to Engine Rotor Fragment Impact", MIT ASRL TR 154-9, March 1976. (Available as NASA CR-134907.)

5. Wu, R.W.-H., Stagliano, T.R., Witmer, E.A. and Spilker, R.L., "User's Guide to Computer Programs JET 5A and CIVM-JET 5B to Calculate the Large Elastic-Plastic Dynamically-Induced Deformations of Multilayer Partial and/or Complete Structural Rings", MIT ASRL TR 154-10, February 1977.

6. Wu, R.W.-H. and Witmer, E.A., "Finite Element Predictions of Transient Elastic-Plastic Large Deflections of Stiffened and/or Unstiffened Rings and Cylindrical Shells", AMMRC CTR 74-31 (also MIT ASRL TR 171-4), April 1974.

7. Pirotin, S.D., Berg, B.A. and Witmer, E.A., "PETROS 3.5: New Developments and Program Manual for the Finite-Difference Calculation of Large Elastic-Plastic Transient Deformations of Multilayer Variable-Thickness Shells", BRL CR 211 (MIT ASRL TR 152-4), February 1975.

8. Santiago, J.M., Wisniewski, H.L. and Huffington, N.J. Jr., "A User's Manual for the REPSIL Code", BRL Report No. 1744, October 1974 (AD A003176).

9. Spilker, R.L., Witmer, E.A. and French, S.E., "Finite Element Nonlinear Transient Response Analysis of Panels Subjected to Impulse or Impact Loads", MIT ASRL TR 154-13 (in preparation).

10. Private Communication from A. Martino, U.S. Naval Air Propulsion Test Center, Phila, Pa., 1970.

11. Mangano, G.J., "Rotor Burst Protection Program -- Phases VI and VII: Exploratory Experimentation to Provide Data for the Design of Rotor Burst Fragment Containment Rings", NAPTC-AED-1968, March 1972. (Available as NASA CR-120962).

12. --- "Rotor Burst Protection Program". (Study for NASA Lewis Research Center on NASA DPR-105 and NASA Interagency Agreement C-41581-B), U.S. Naval Air Propulsion Test Center, Aeronautical Engine Dept., Progress Reports Sept. 1969 - Jan. 1977.

13. Private communications from G.J. Mangano, R. DeLucia, and J. Salvino, U.S. Naval Air Propulsion Test Center, Trenton, New Jersey 1975-1976.

14. Witmer, E.A., Merlis, F. and Spilker, R.L., "Experimental Transient and Permanent Deformation Studies of Steel-Sphere-Impacted or Impulsively-Loaded Aluminum Beams with Clamped Ends", MIT ASRL TR 154-11, October 1975. (Available as NASA CR-134922.)

15. Witmer, E.A., Merlis, F., Rodal, J.J.A. and Stagliano, T.R., "Experimental Transient and Permanent Deformation Studies of Steel-Sphere-Impacted or Impulsively-Loaded Aluminum Panels", MIT ASRL TR 154-12, March 1977.

16. Balmer, H.A. and Witmer, E.A., "Theoretical-Experimental Correlation of Large Dynamic and Permanent Deformations of Impulsively-Loaded Simple Structures", MIT, AFFDL-TDR-64-108, July 1964.

17. Wu, R.W.-H. and Witmer, E.A., "Finite-Element Analysis of Large Transient Elastic-Plastic Deformations of Simple Structures, with Application to the Engine Rotor Fragment Containment/Deflection Problem", ASRL TR 154-4, Aeroelastic and Structures Research Laboratory, Massachusetts Institute of Technology, January 1972. (Available as NASA CR-120886.)

18. Collins, T.P. and Witmer, E.A., "Application of the Collision-Imparted Velocity Method for Analyzing the Responses of Containment and Deflector Structures to Engine Rotor Fragment Impact", MIT ASRL TR 154-8, August 1973. (Available as NASA CR-134494.)

19. Zirin, R.M. and Witmer, E.A., "Examination of the Collision Force Method for Analyzing the Responses of Simple Containment/Deflection Structures to Impact by One Engine Rotor Blade Fragment", ASRL TR 154-6, Aeroelastic and Structures Research Laboratory, Massachusetts Institute of Technology, May 1972. (Available as NASA CR-120952.)

TABLE 1

DATA CHARACTERIZING NAPTC RING TEST 91

Ring Data	Test 91
Outside Diameter (in)	17.619
Radial Thickness (in)	0.152
Axial Length (in)	1.506
Material	2024-T4
Elastic Modulus E (psi)	10^7
PP Yield Stress σ_o (psi)	50,000

Fragment Data	
Type	T-58 Single Blade
Material	SEL-15
Outer Radius (in)	7.0
Fragment Centroid from Center of Rotation (in)	4.812
Fragment Tip Clearance from Ring (in)	1.658
Fragment Length (in)	3.5
Fragment Length from CG to Tip (in)	2.188
Fragment Weight (lbs)	0.084
Fragment Moment of Inertia about its CG (in lb sec^2)	2.163×10^{-4}
Failure Speed (RPM)	15,644.4
Fragment Tip Velocity (ips)	11,467.
Fragment Centroidal Velocity (ips)	7,884.
Fragment Initial Angular Velocity (rad/sec)	1,638.3
Fragment Translation KE (in lb)	6,756.
Fragment Rotational KE (in lb)	290.3

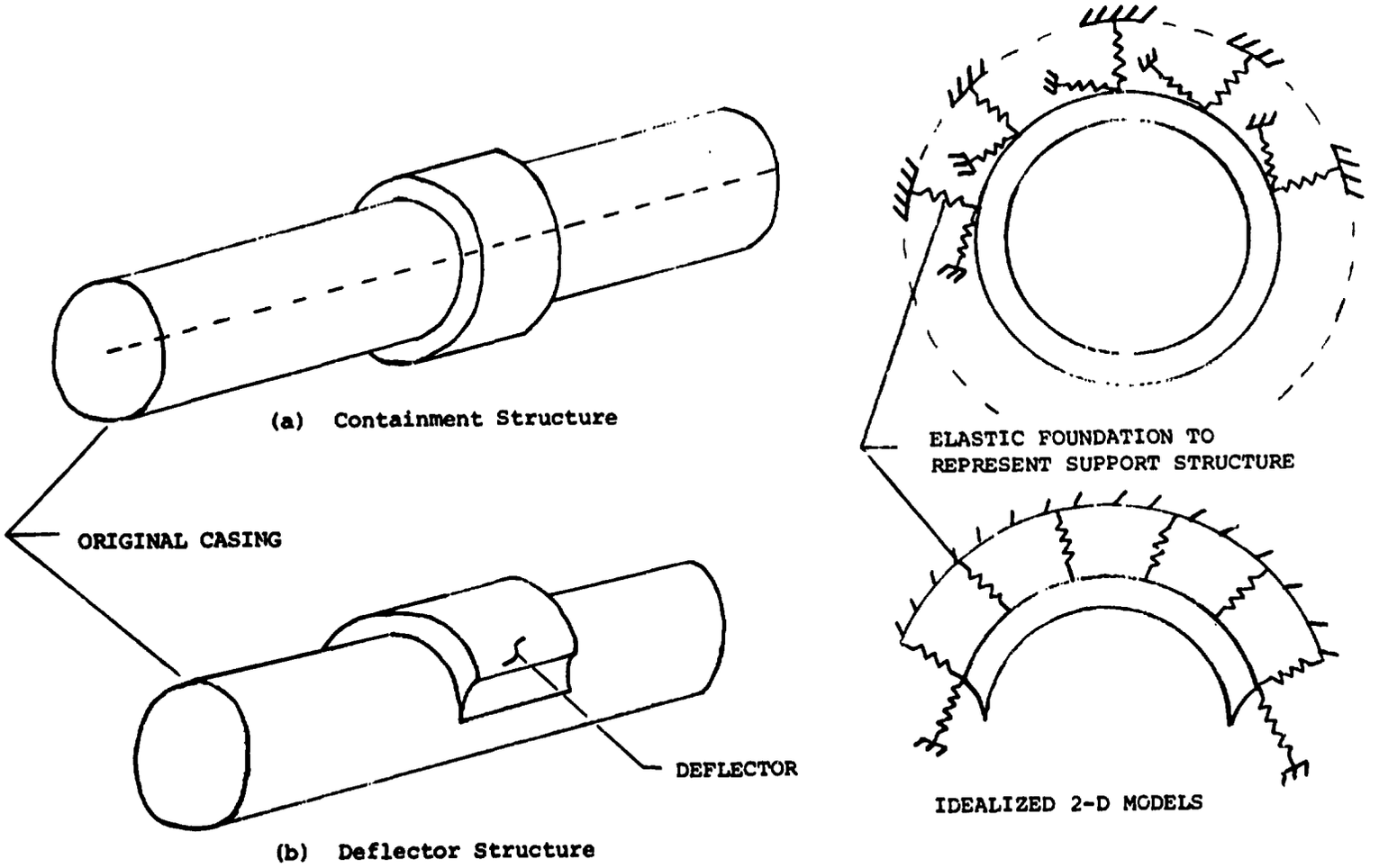

FIG. 1 SCHEMATICS OF CONTAINMENT AND DEFLECTOR STRUCTURES, AND ASSOCIATED IDEALIZED 2-D STRUCTURAL MODELS

- DEVELOPMENT OF PREDICTION METHODS FOR STRUCTURAL RESPONSE
  - TO PRESCRIBED TRANSIENT LOADS OR INITIAL VELOCITIES → JET CODES (FINITE ELEMENT)
  - TO FRAGMENT IMPACT → CIVM-JET CODES
  - ANALYSIS OF 2-D STRUCTURES
    - SINGLE-LAYER RINGS → NEAR COMPLETION
    - MULTILAYER RINGS → IN PROGRESS
  - ANALYSIS OF GENERAL PANEL RESPONSE
    - SINGLE LAYER → IN PROGRESS
    - MULTILAYER → NEXT

- EXPERIMENTS
  - SMALL SCALE SIMPLIFIED IMPACT TESTS AT MIT TO SUPPLEMENT COMPLEX FULL-SCALE TEST AT THE NAPTC
    - OBTAIN DATA TO MAKE IN-DETAIL EVALUATION OF ADEQUACY OF PREDICTION METHOD
    - IMPACT OF STEEL SPHERE AGAINST
      - BEAMS
      - FLAT SINGLE-LAYER PANELS
      - WAFFLE-STIFFENED PANELS

      } CLAMPED EDGES

- THEORETICAL-EXPERIMENTAL CORRELATION STUDIES
  - USE OF MIT-ASRL EXPERIMENTS
  - USE OF NAPTC DATA

- COMPUTER CODES
  - PARAMETRIC AND SCREENING STUDIES
  - TO ASSIST PRELIMINARY DESIGN OF CONTAINERS AND DEFLECTORS

FIG. 2 SUMMARY OF MIT-ASRL STUDIES ON ENGINE ROTOR FRAGMENT IMPACT ON C/D STRUCTURES

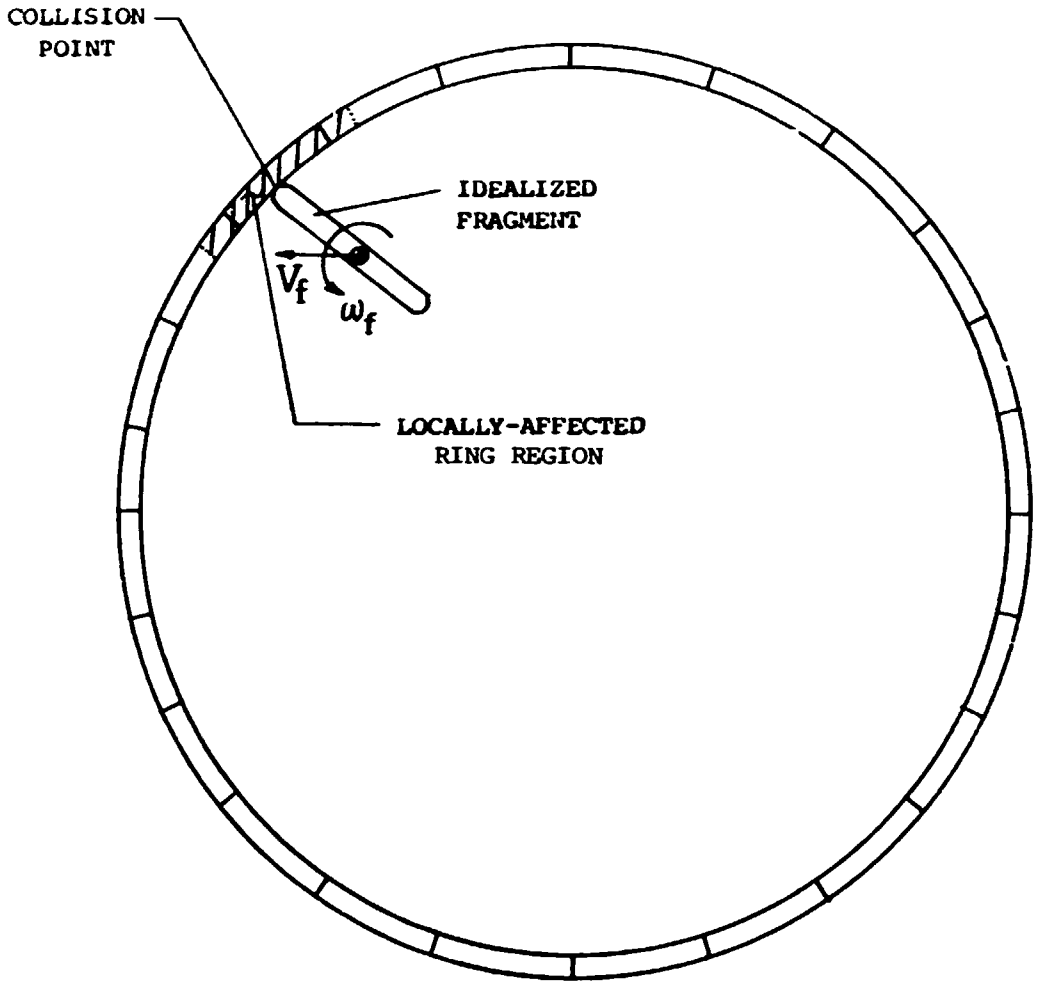

FIG. 3 SCHEMATIC OF A CONTAINMENT RING SUBJECTED TO SINGLE-FRAGMENT IMPACT

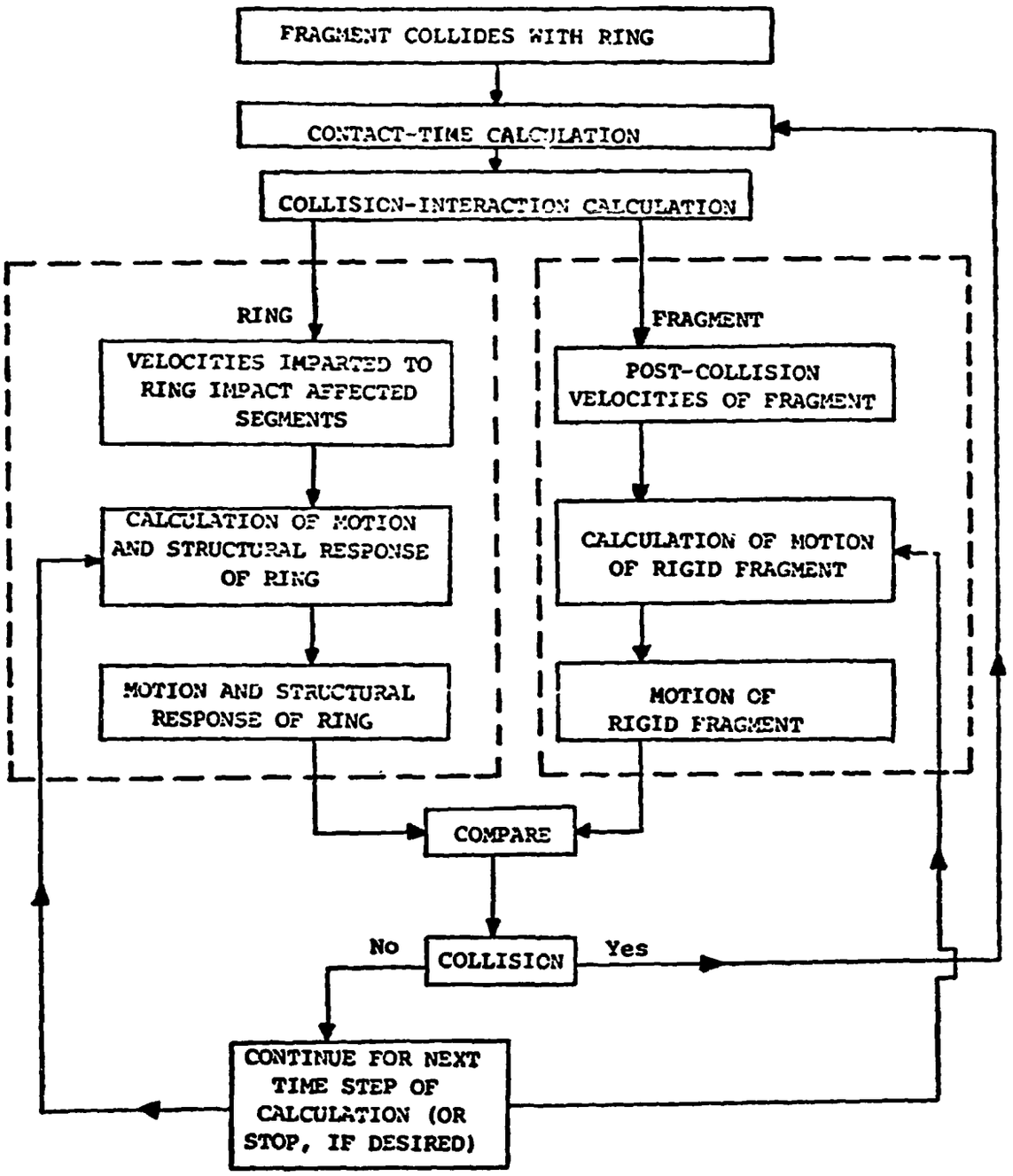

FIG. 4 INFORMATION FLOW SCHEMATIC FOR PREDICTING RING AND FRAGMENT MOTIONS IN THE COLLISION-IMPARTED VELOCITY METHOD

o —·— EXPERIMENT

x ----- CASE CR-11B (EL-PP-SR, e = 0)

Δ —— CASE CR-10B (EL-PP-SR, e = 1)

——— RING BEFORE INITIAL IMPACT

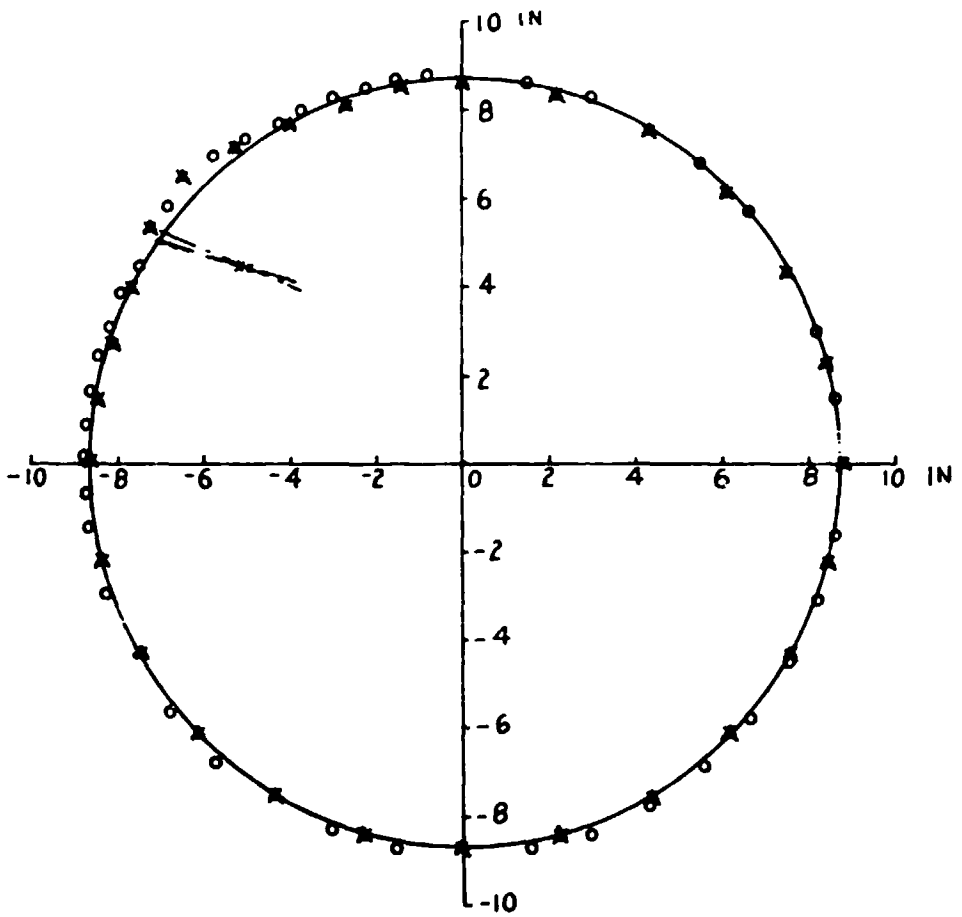

(a) TAII = 150 μsec

FIG. 5 COMPARISON OF CIVM PREDICTIONS WITH EXPERIMENT FOR THE FREE COMPLETE RING SUBJECTED TO SINGLE-BLADE IMPACT IN NAPTC TEST 91

o —·— EXPERIMENT

x ---- CASE CR-11B (EL-PP-SR, e = 0)

Δ —— CASE CR-10B (EL-PP-SR, e = 1)

——— RING BEFORE INITIAL IMPACT

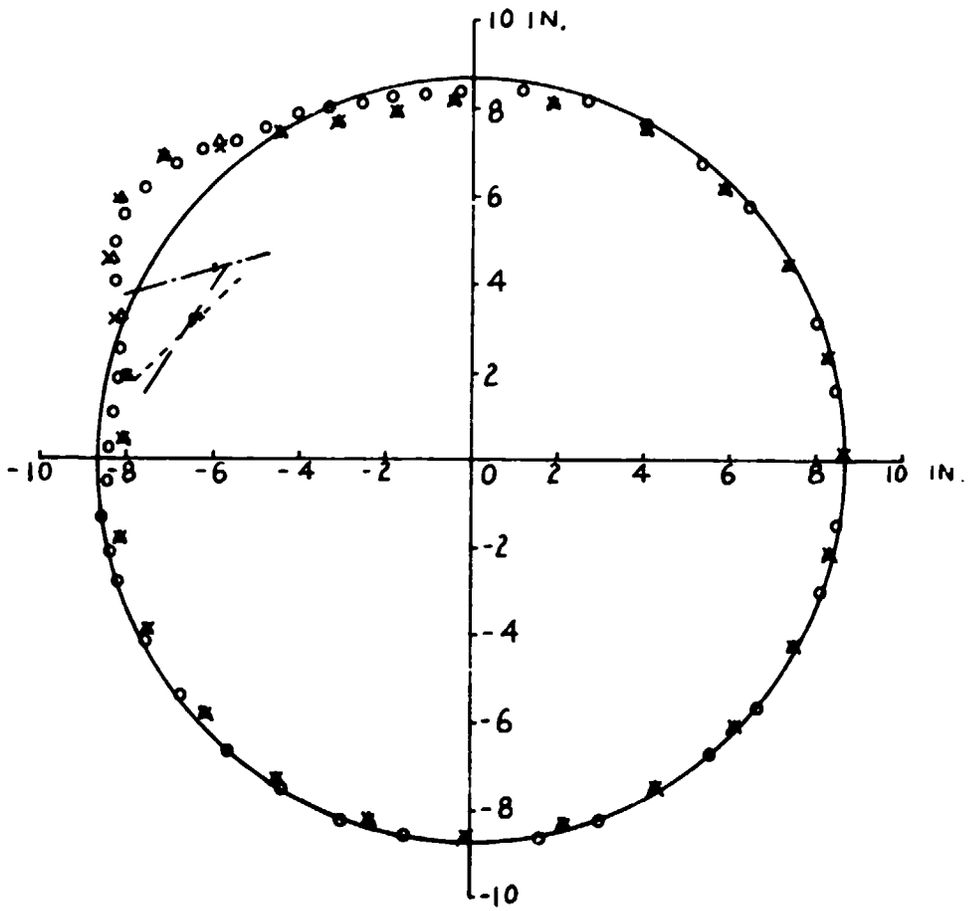

(b) TAII = 570 μsec

FIG. 5 CONTINUED

o — · — EXPERIMENT

x - - - - CASE CR-11B (EL-PP-SR, e = 0)

Δ — — CASE CR-10B (EL-PP-SR, e = 1)

——— RING BEFORE INITIAL IMPACT

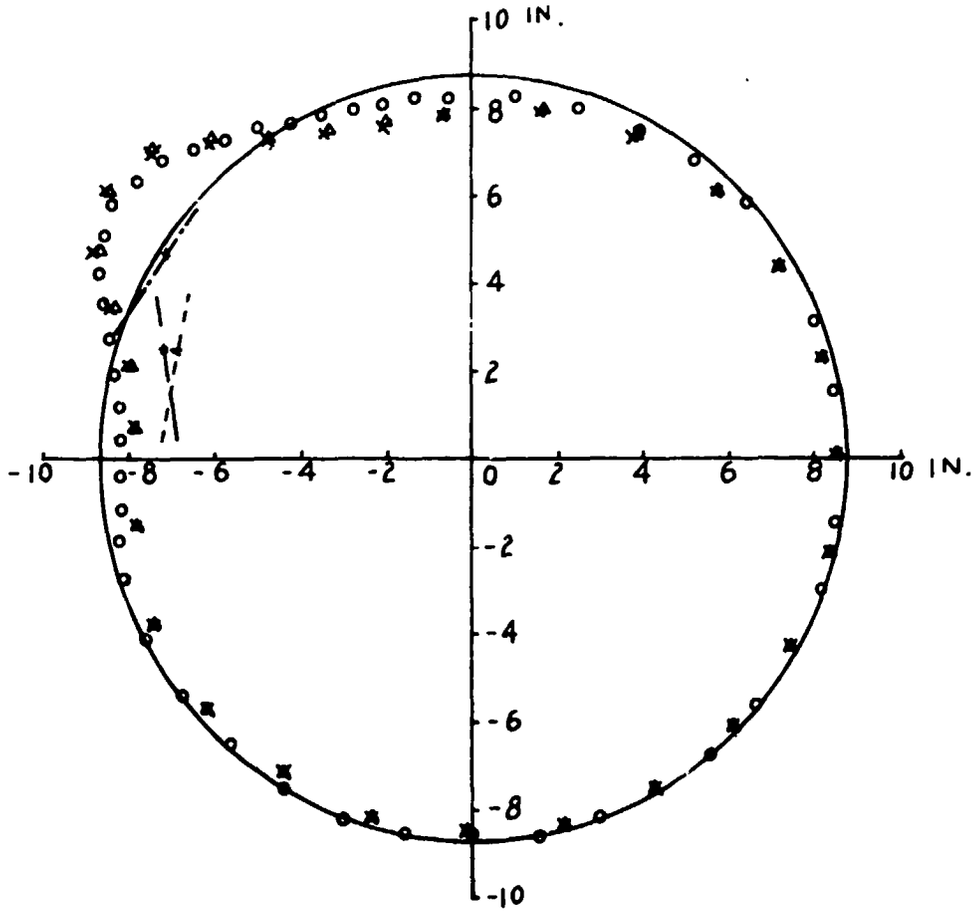

(c) TAII = 810 μsec

FIG. 5 CONCLUDED

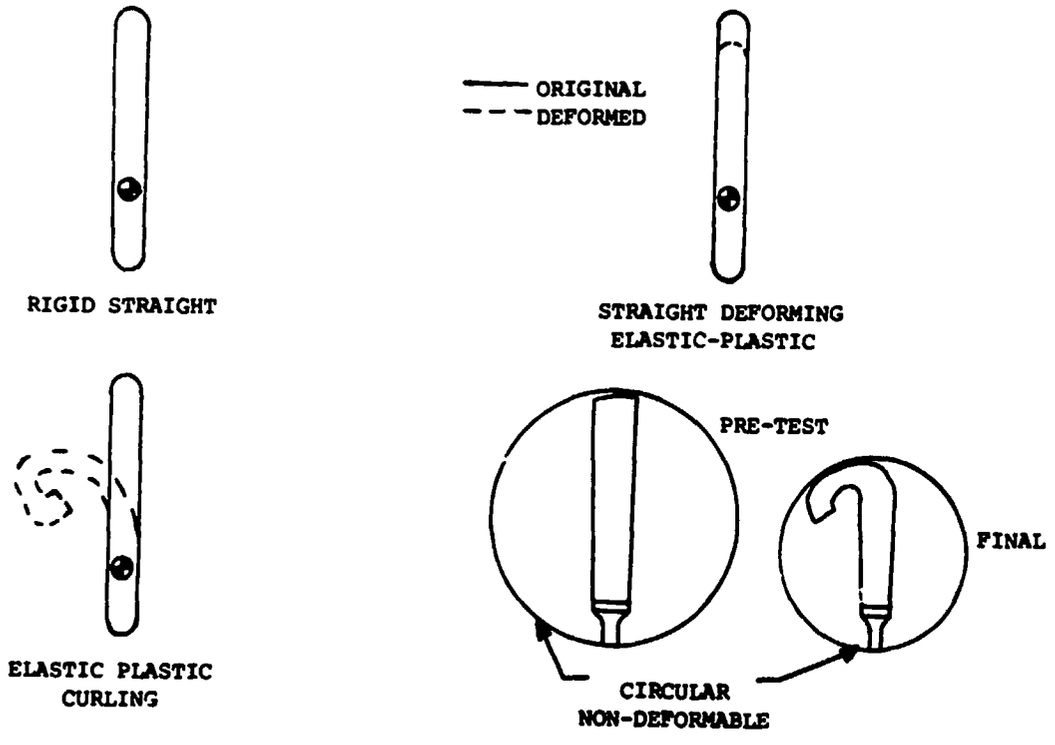

FIG. 6 SCHEMATICS OF ACTUAL AND IDEALIZED FRAGMENTS

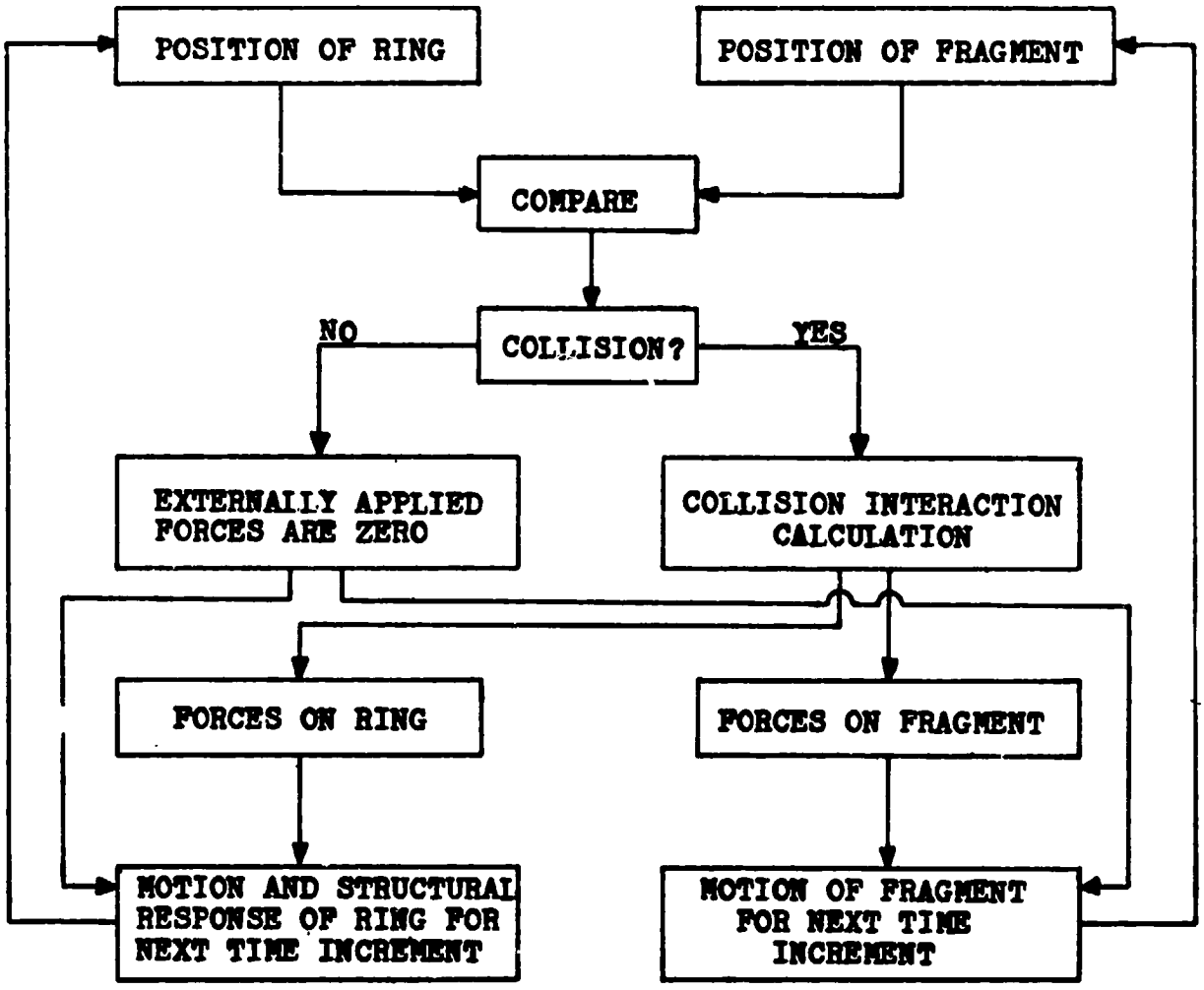

FIG. 7 INFORMATION FLOW SCHEMATIC FOR PREDICTING RING AND FRAGMENT MOTIONS IN THE COLLISION FORCE METHOD

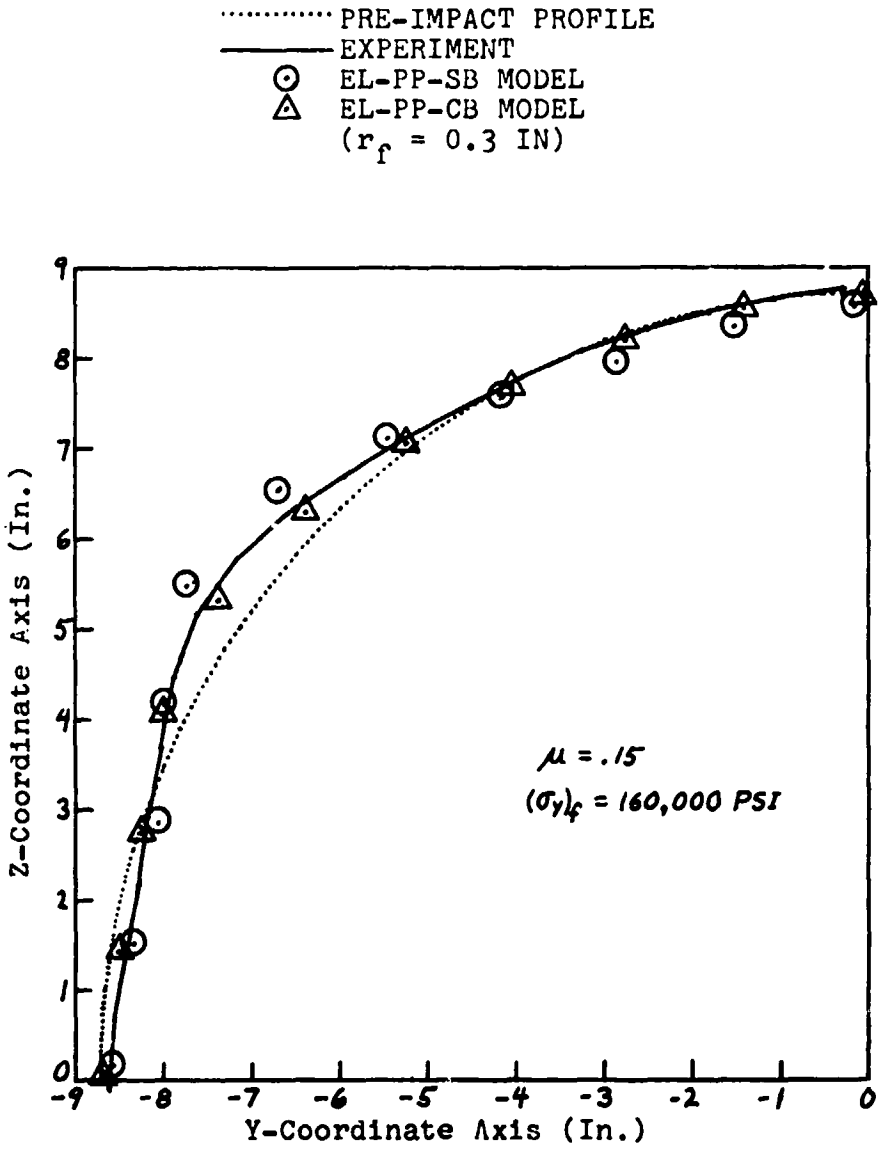

(a) First Quadrant of the Deformed Ring at TAII = 326 μsec.

FIG. 8 COMPARISON OF CFM PREDICTIONS FOR EL-PP-SB AND EL-PP-CB BLADE MODELS FOR μ=.15 BLADE/RING IMPACT VERSUS EXPERIMENTAL DEFORMED RING DATA

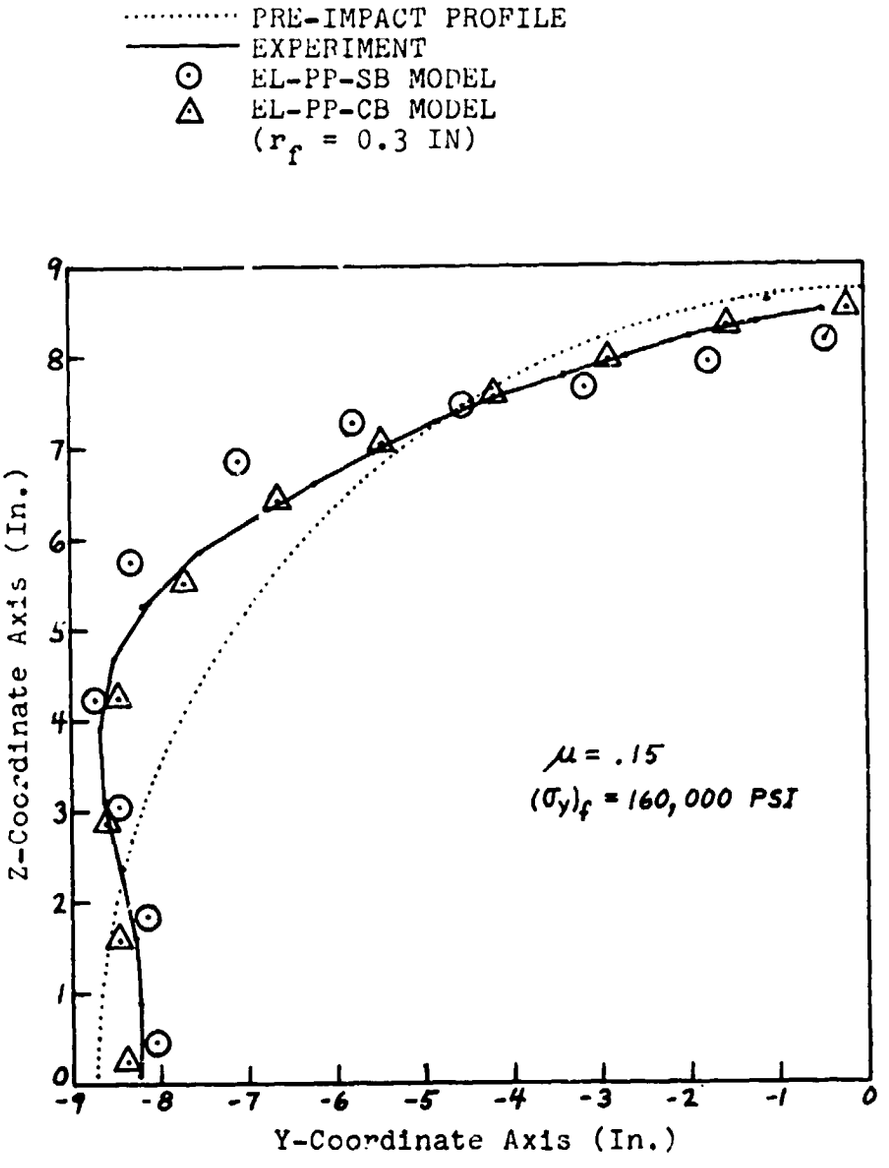

(b) First Quadrant of the Deformed Ring at TAII = 626 μsec.

FIG. 8 CONCLUDED

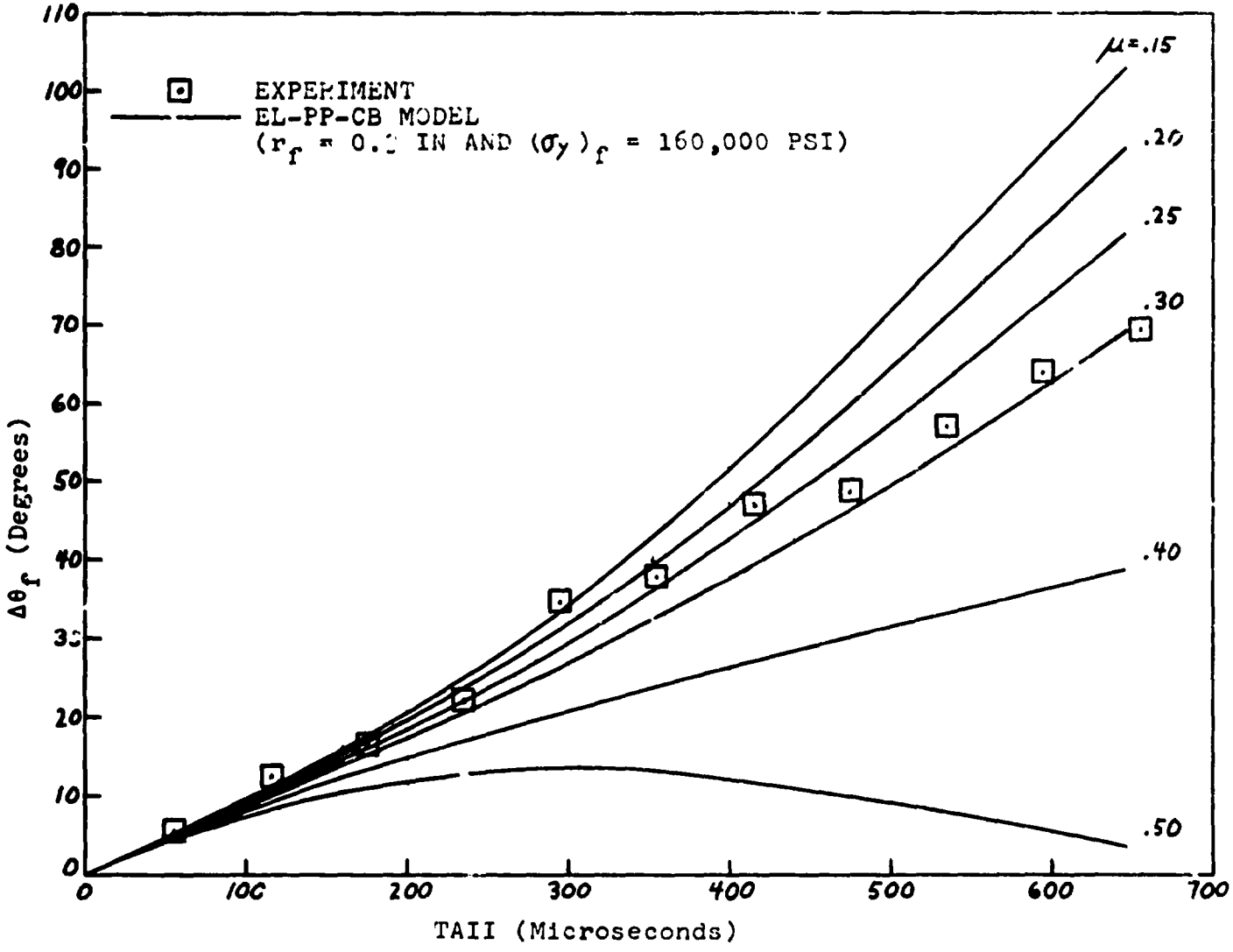

FIG. 9 COMPARISON OF CFM PREDICTIONS OF BLADE MOTION FOR THE EL-PP-CB BLADE MODEL AND VARIOUS VALUES OF THE FRICTION COEFFICIENT μ VERSUS OBSERVED BLADE ANGULAR ROTATION

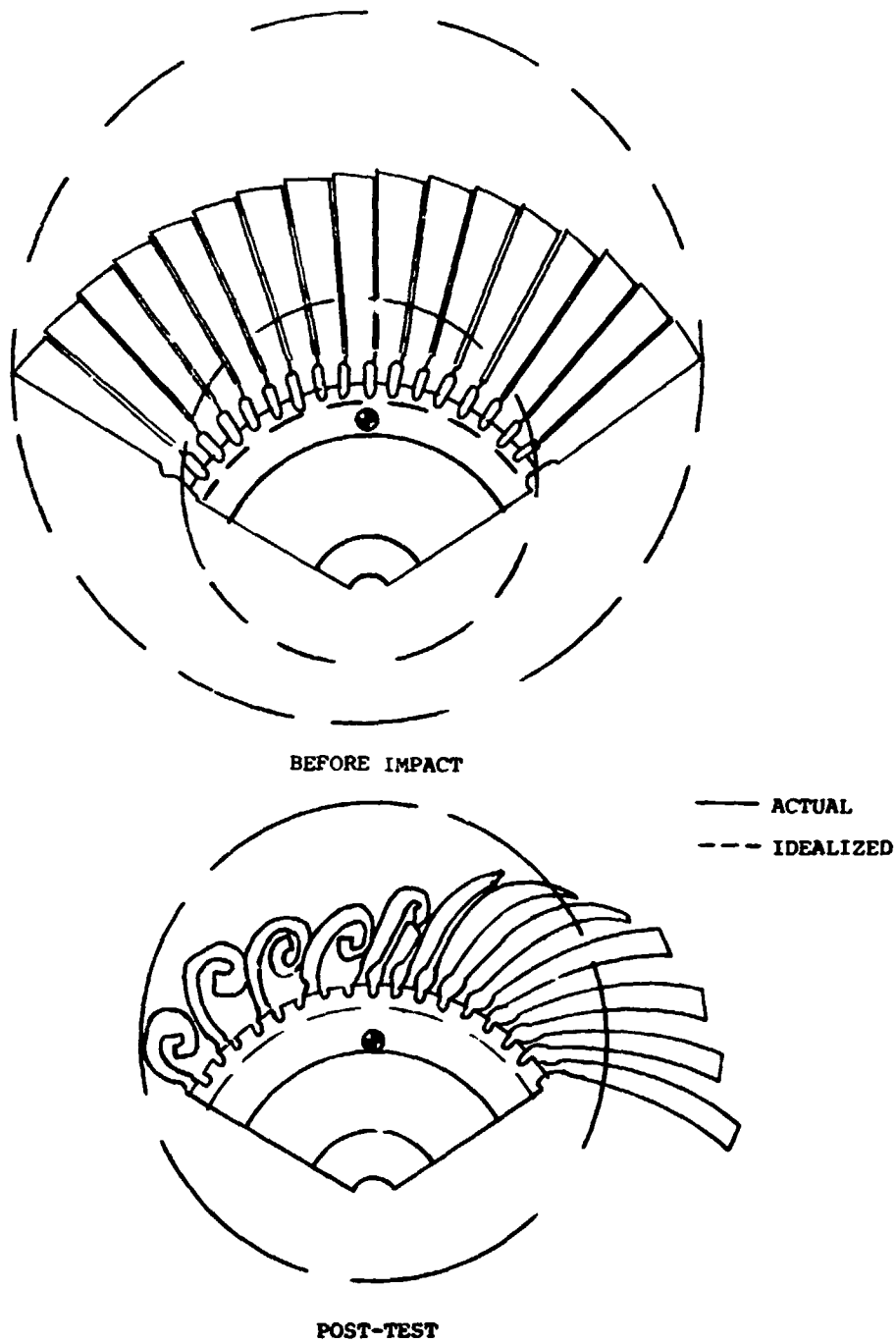

FIG. 10 SCHEMATICS OF PRE-TEST AND DEFORMED TRI-HUB DISK/BLADE FRAGMENTS, AND IDEALIZED MODELS

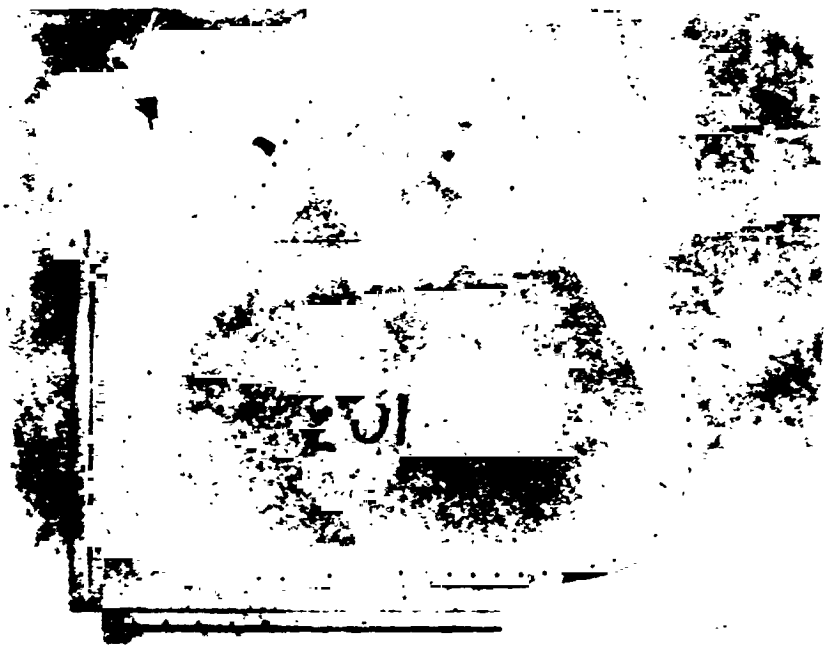

FIG. 11 POST-TEST CONFIGURATION OF THE STEEL CONTAINMENT RING SUBJECTED TO T58 TURBINE ROTOR TRI-HUB BURST IN NAPTC TEST 201

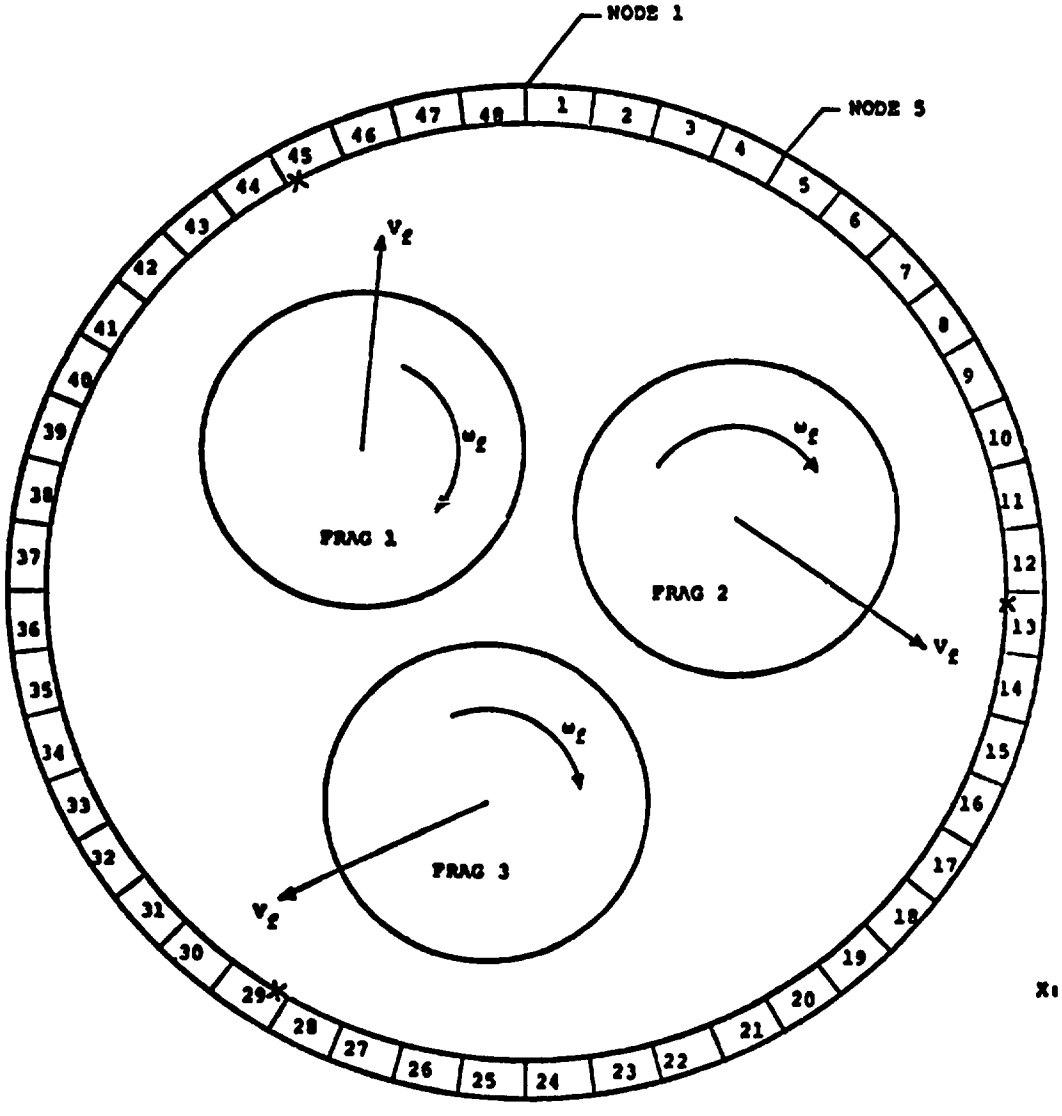

4130 STEEL RING

INNER RADIUS = 7.50 IN
THICKNESS = 0.625 IN
AXIAL LENGTH = 1.50 IN

FINITE-ELEMENT ANALYSIS

48 EQUAL ELEMS (FULL RING)
4 DOF/NODE
EL-SH-SR

FRAGMENTS: 3 EQUAL CIRCULAR
AT 120-DEG. SPACING

FOR EACH FRAGMENT

RADIUS = 2.555 IN
MASS = 0.009395 (LB-SEC^2)/IN
MASS MOM. INER. = 0.06899 IN-LB-SEC^2
TRANSL. VEL., V_f = 5816.7 IN/SEC
ROT. VEL., ω_f = 2079.6 RAD/SEC
INITIAL KINETIC ENERGY
TRANSLATIONAL = 158,942 IN-LB
ROTATIONAL = 149,177 IN-LB
TOTAL = 308,119 IN-LB

X: POINT OF INITIAL IMPACT

FIG. 12 GEOMETRIC, TEST, AND MODELING DATA FOR THE 4130 STEEL CONTAINMENT RING SUBJECTED TO TRI-HUB T58 ROTOR BURST IN NAPTC TEST 201

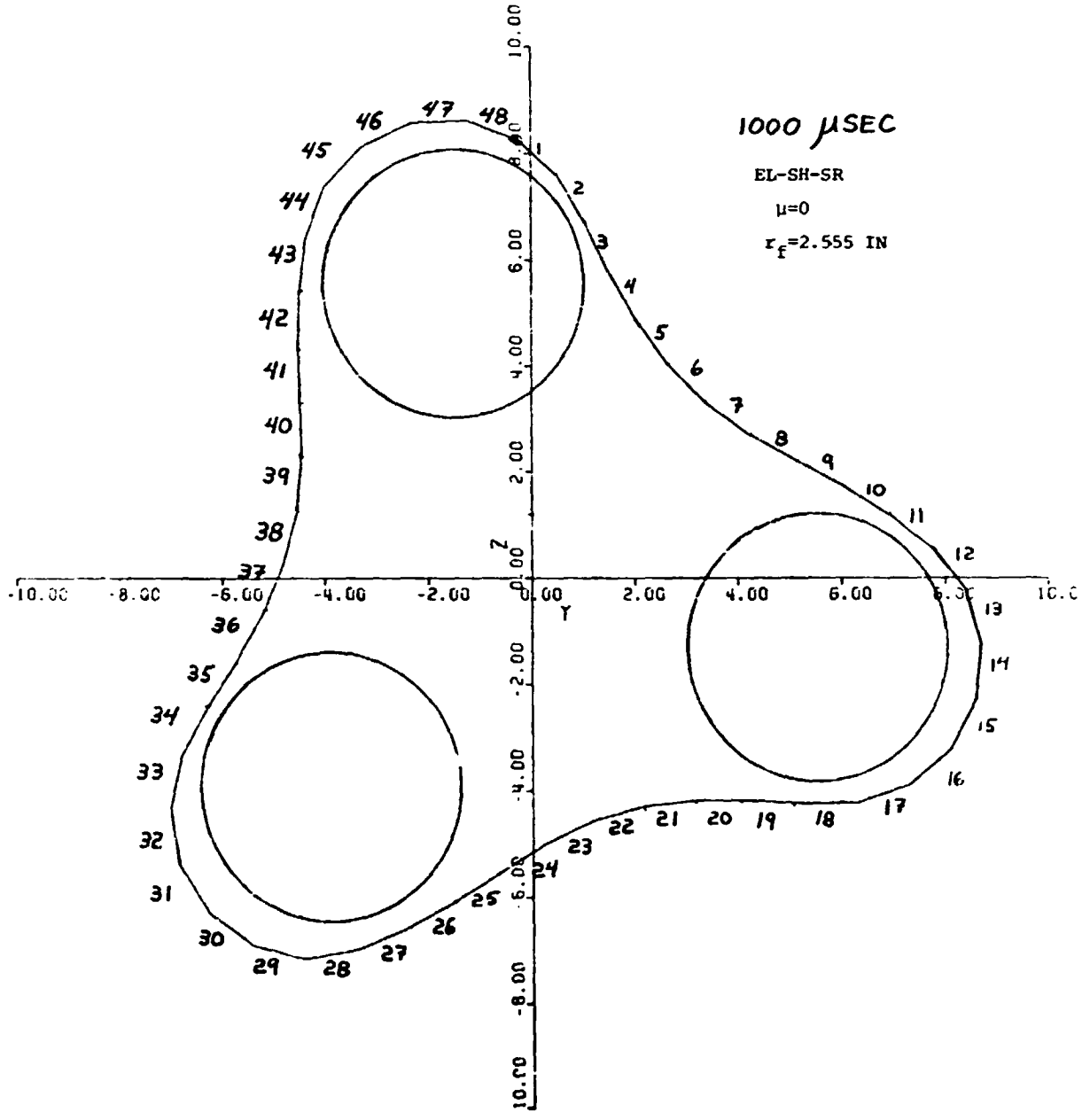

FIG. 13 PREDICTED DEFORMED RING CONFIGURATION AT 1000 MICROSECONDS AFTER INITIAL IMPACT FOR THE NAPTC TEST 201 CONTAINMENT RING

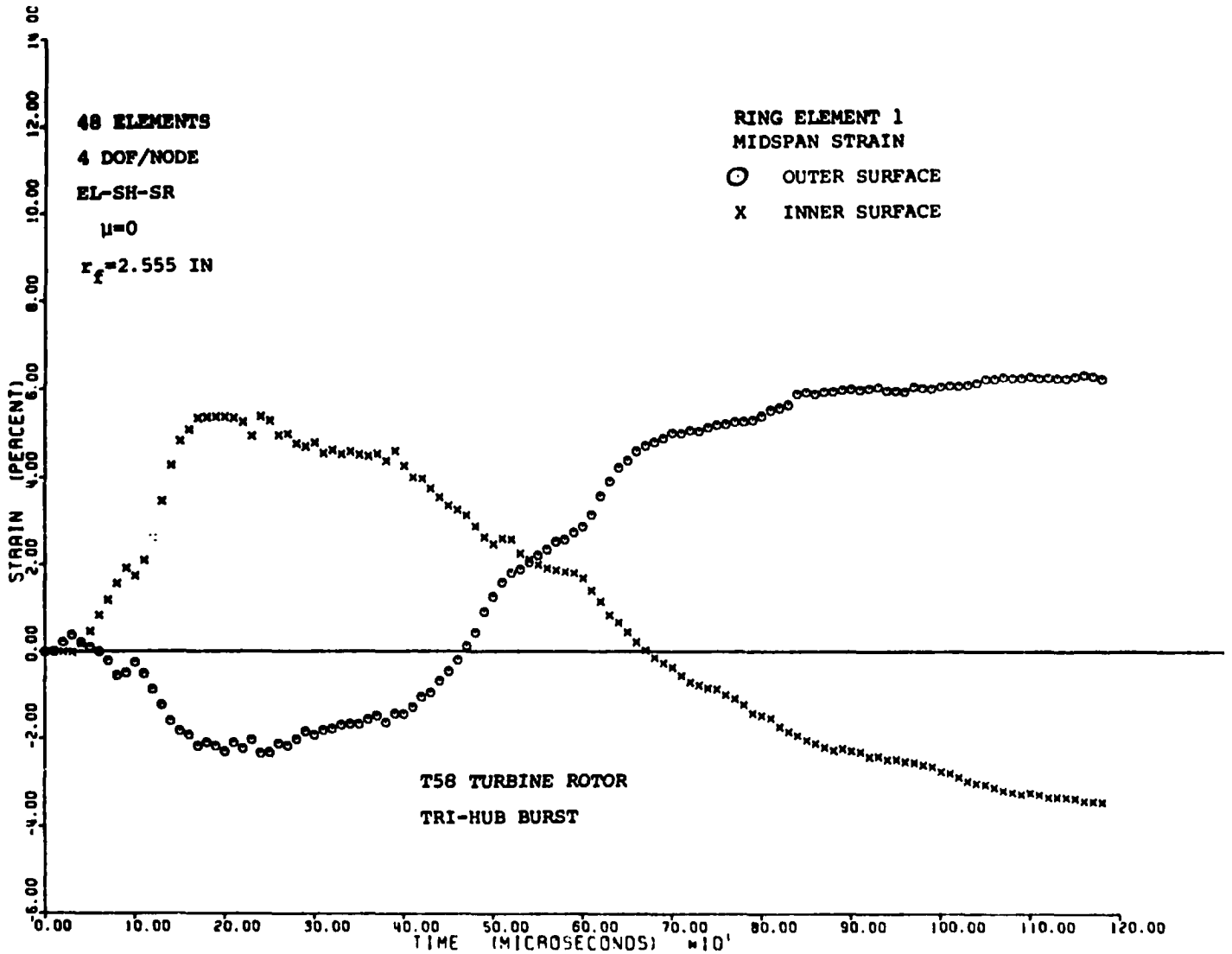

(a) Element 1 Midspan Strain

FIG. 14 PREDICTED TRANSIENT STRAIN ON THE NAPTC TEST 201 CONTAINMENT RING

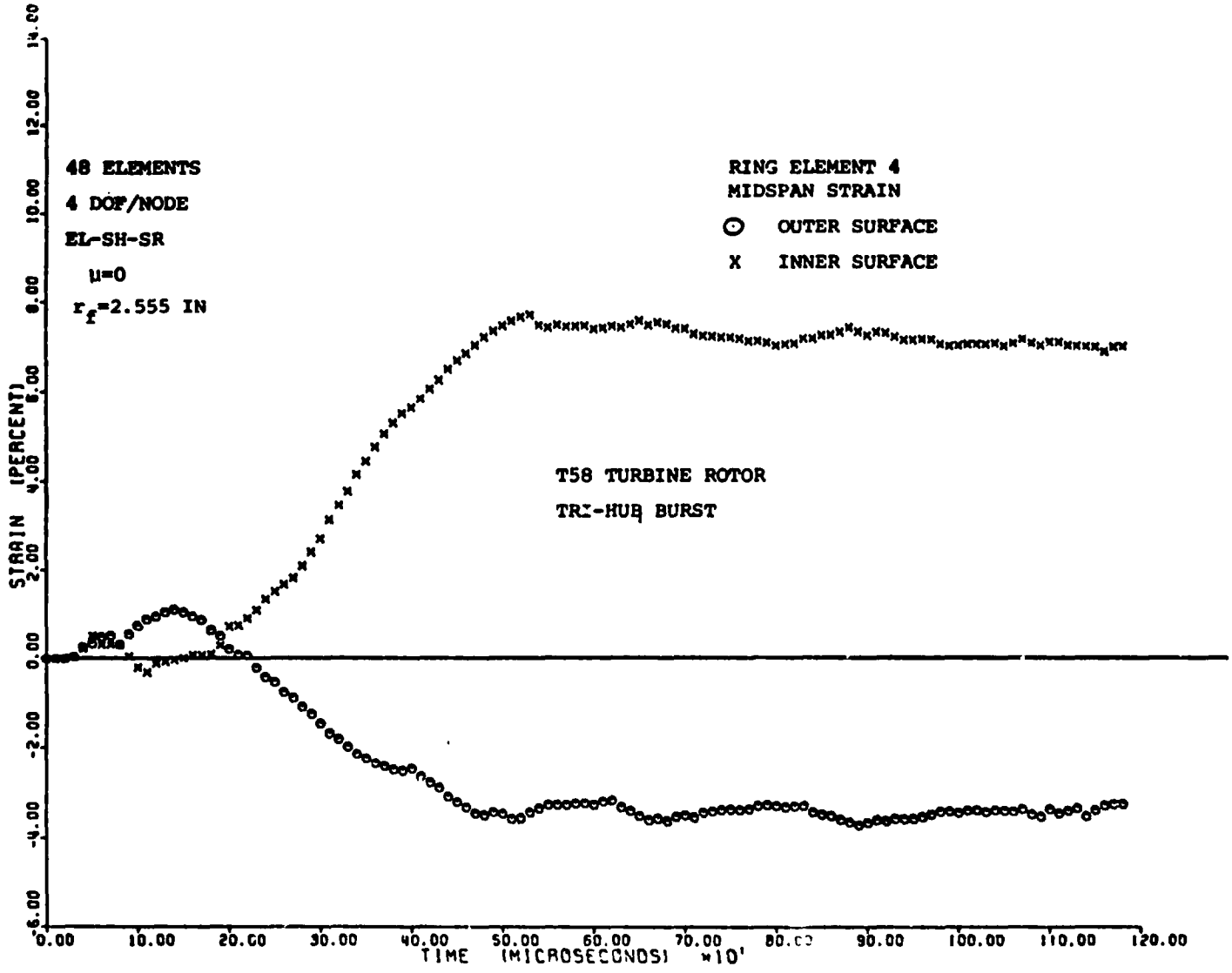

(b) Element 4 Midspan Strain

FIG. 14 CONTINUED (NAPTC TEST 201 RING)

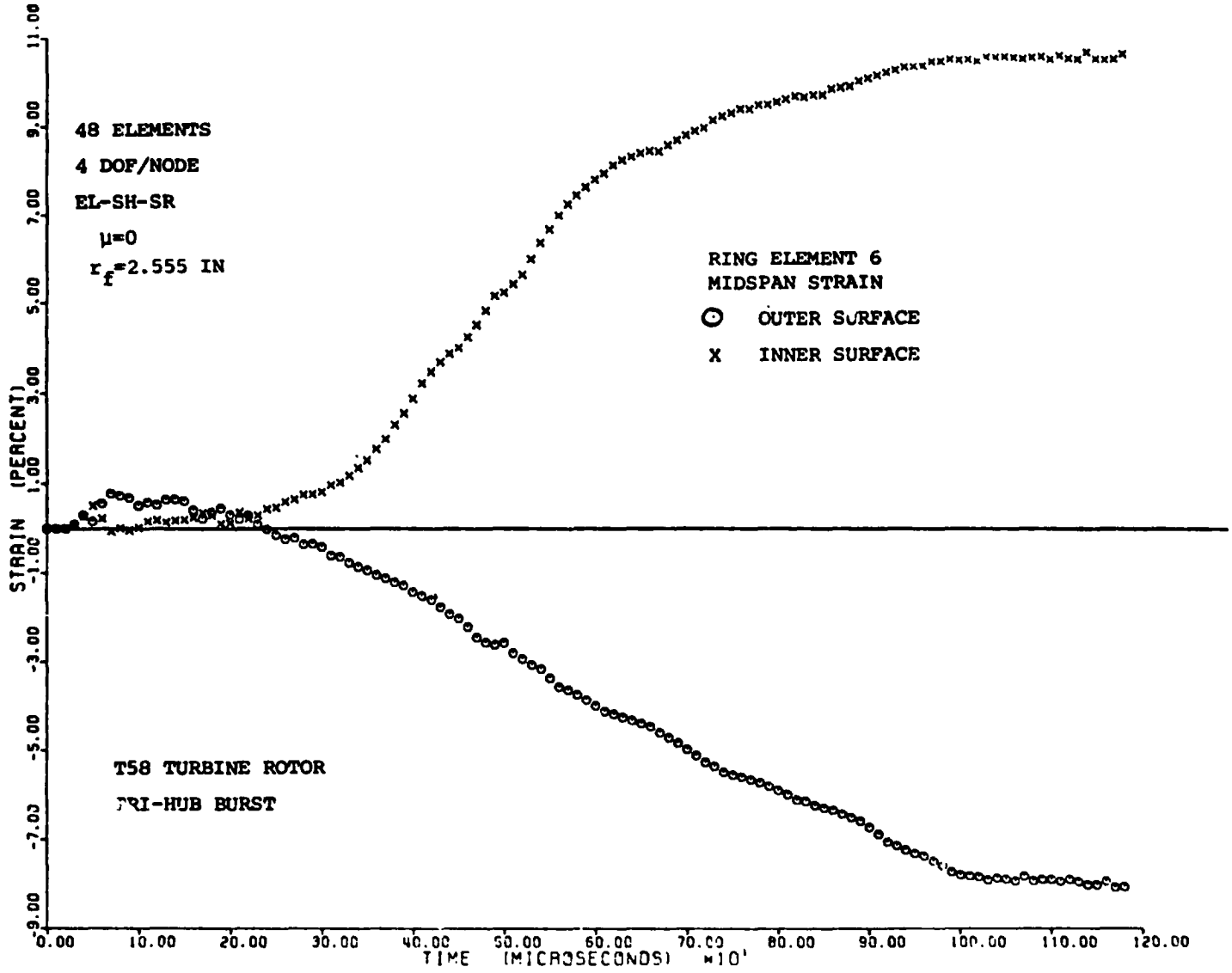

(c) Element 6 Midspan Strain

FIG. 14 CONCLUDED (NAPTC TEST 201 RING)

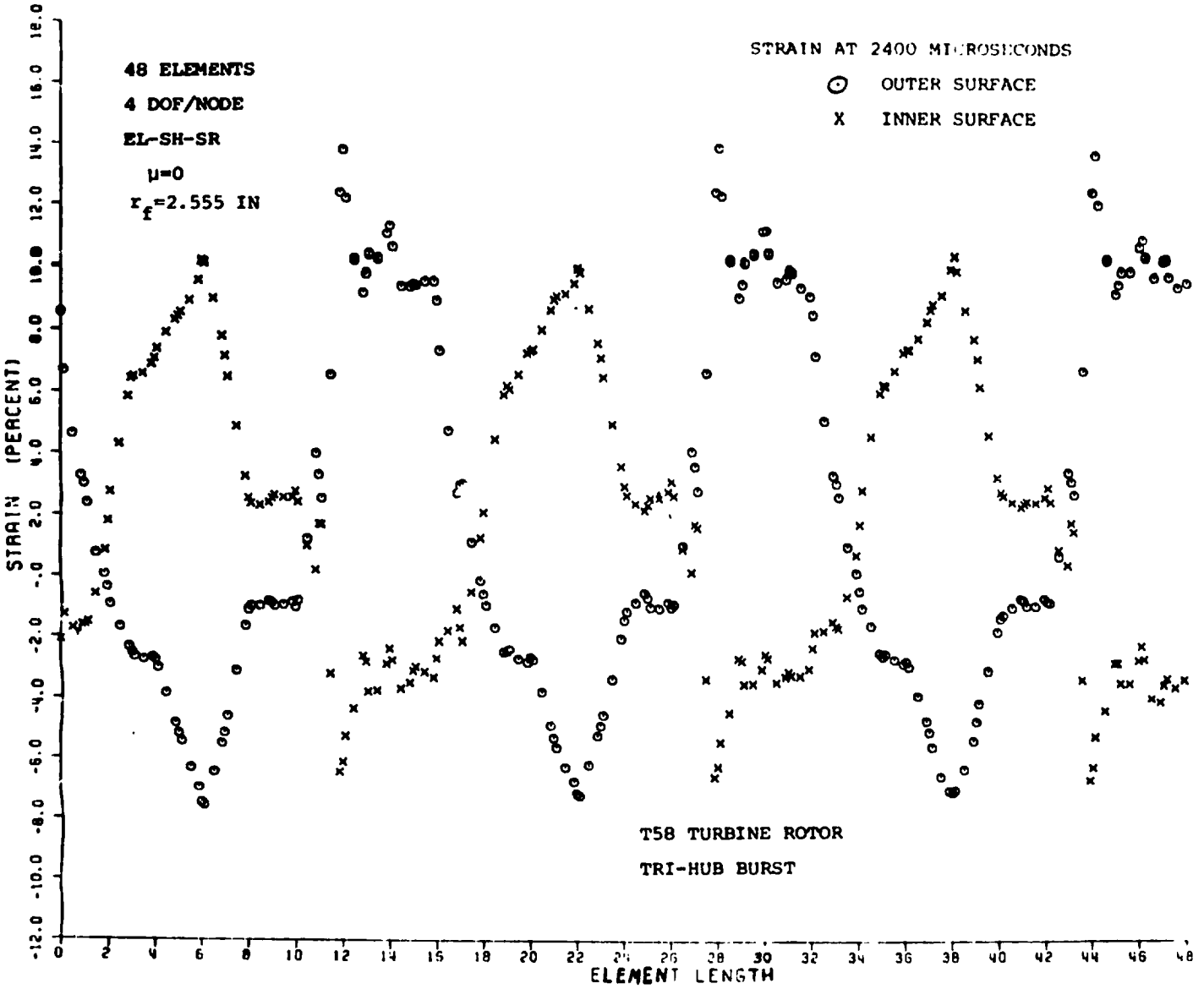

FIG. 15 CIRCUMFERENTIAL DISTRIBUTION OF PREDICTED INNER-SURFACE AND OUTER-SURFACE STRAIN AT 2400 MICROSECONDS AFTER INITIAL IMPACT FOR THE NAPTC TEST 201 CONTAINMENT RING FOR r_f=2.555 IN AND μ=0

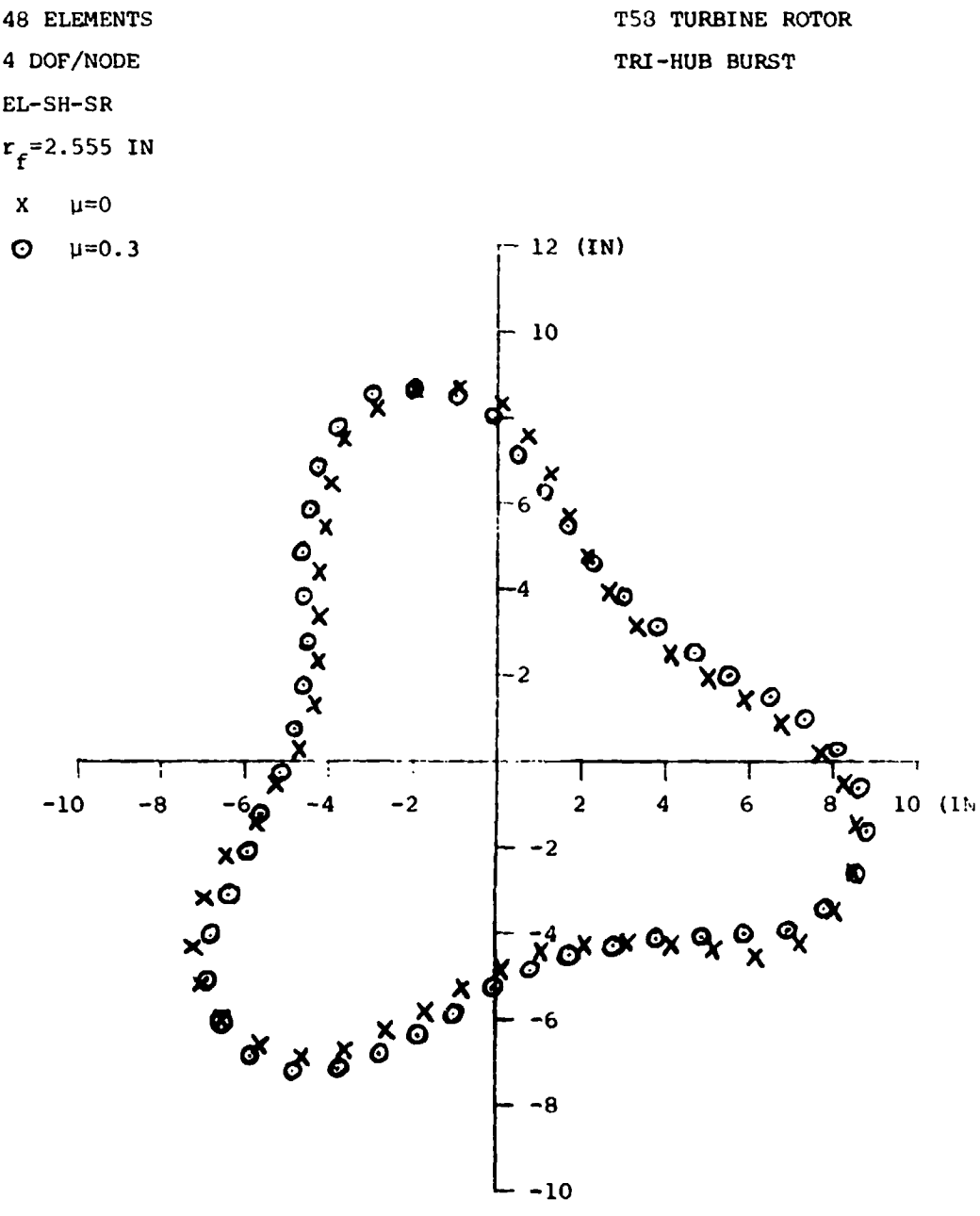

FIG. 16 COMPARISON OF PREDICTED DEFORMED RING CONFIGURATIONS AT 1200 MICROSECONDS AFTER INITIAL IMPACT FOR μ=0 AND μ=0.3 WITH r_f=2.555 IN FOR THE NAPTC TEST 201 CONTAINMENT RING

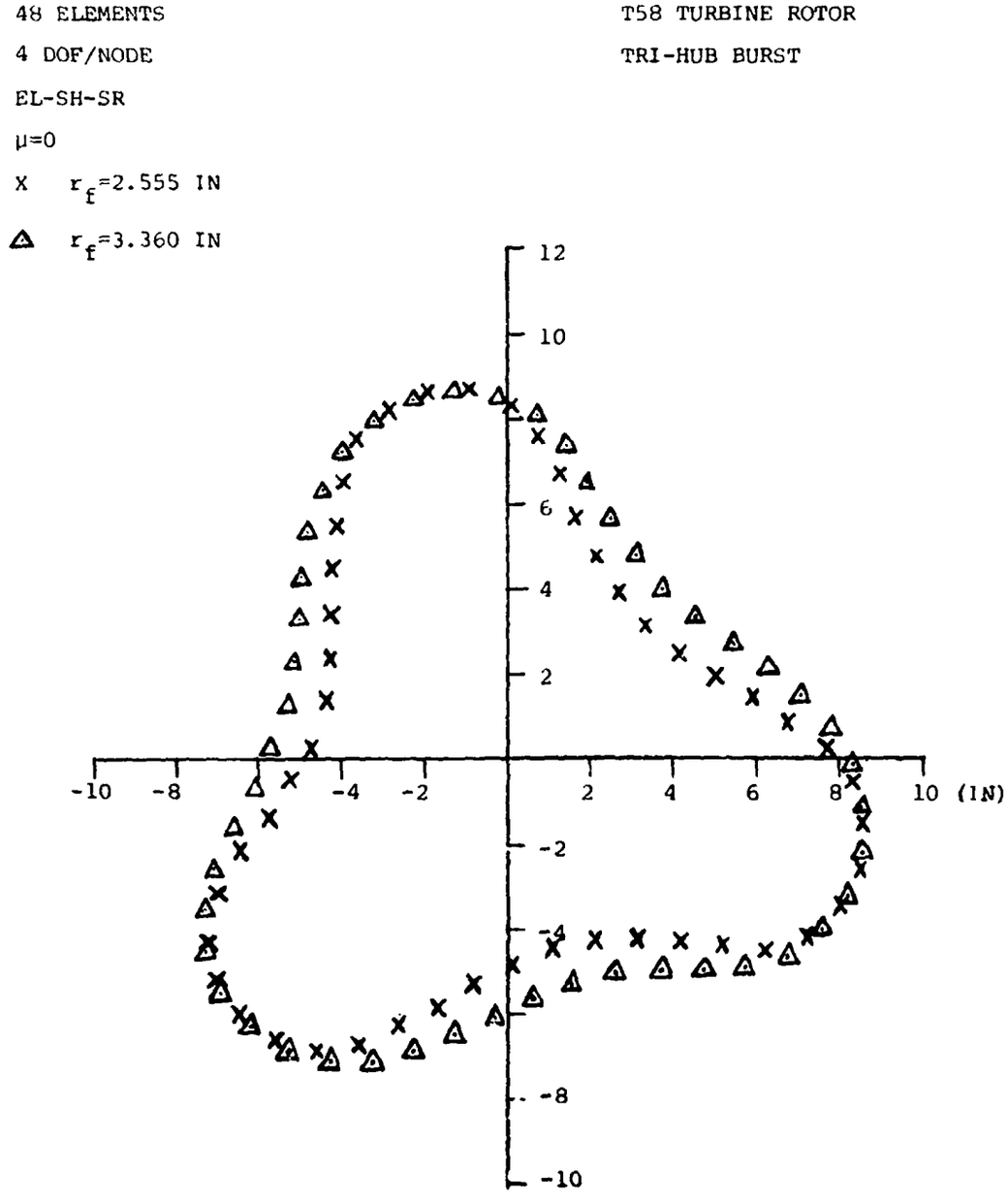

FIG. 17 COMPARISON OF PREDICTED DEFORMED RING CONFIGURATIONS AT 1200 MICROSECONDS AFTER INITIAL IMPACT FOR TWO DIFFERENT FRAGMENT-SIZE MODELINGS AND FRICTIONLESS IMPACT CONDITIONS FOR THE NAPTC TEST 201 CONTAINMENT RING

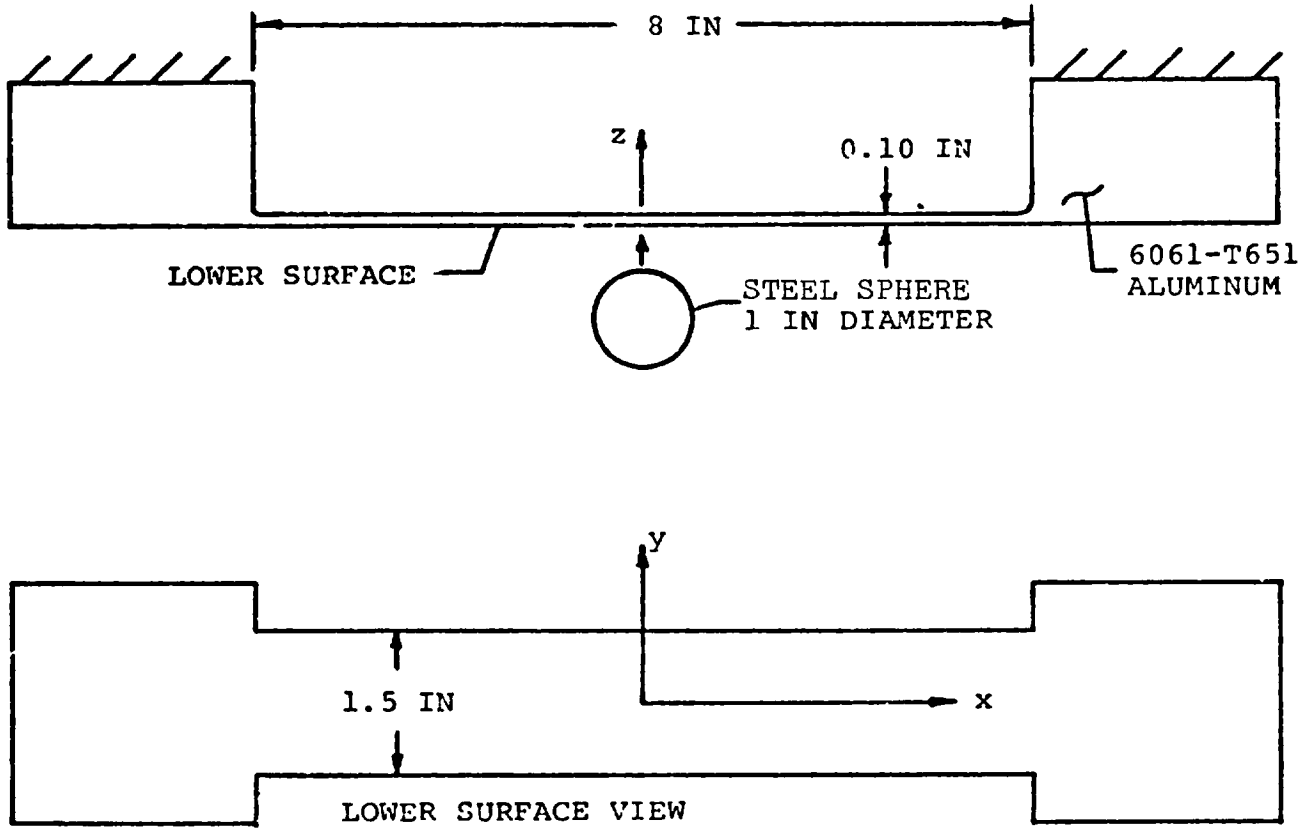

FIG. 18 SCHEMATIC OF 6061-T651 NARROW PLATE OR BEAM MODEL SUBJECTED TO IMPACT BY A ONE-INCH DIAMETER STEEL SPHERE

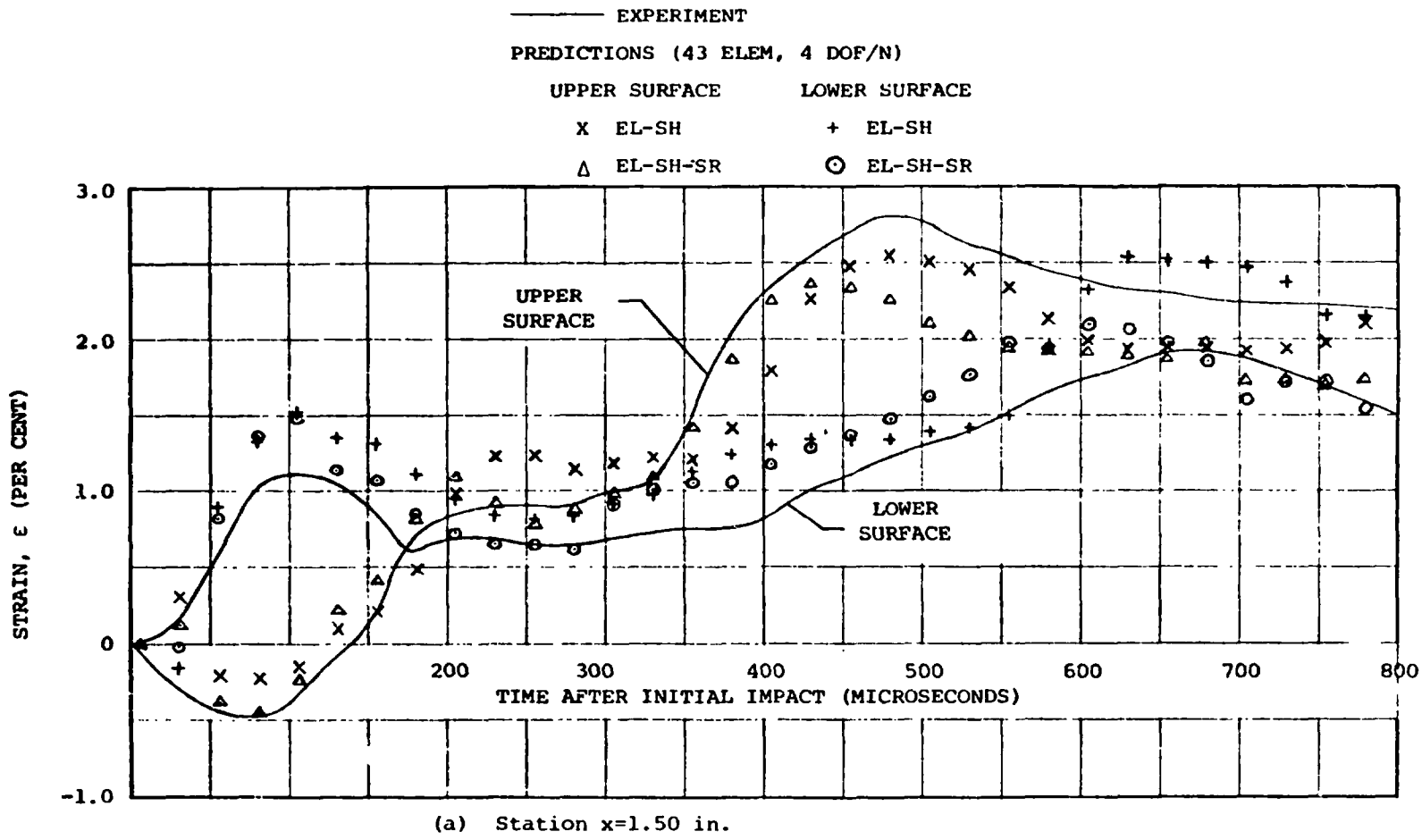

(a) Station x=1.50 in.

FIG. 19 TRANSIENT STRAIN AT VARIOUS SPANWISE STATIONS OF STEEL-SPHERE-IMPACTED 6061-T651 ALUMINUM ⅄ AM MODEL CB-18

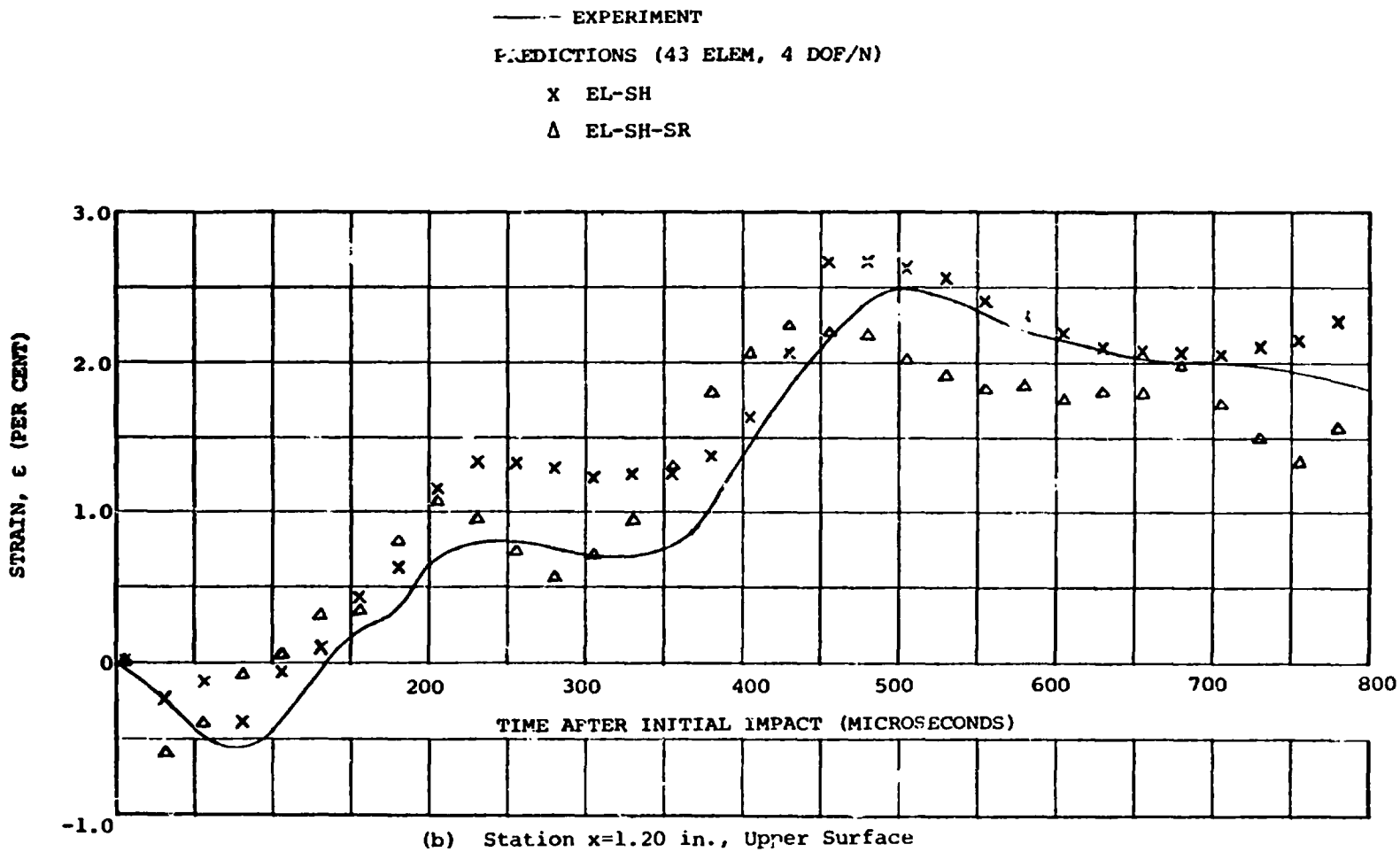

(b) Station x=1.20 in., Upper Surface

FIG. 19 CONCLULED (CB-18)

C-3.

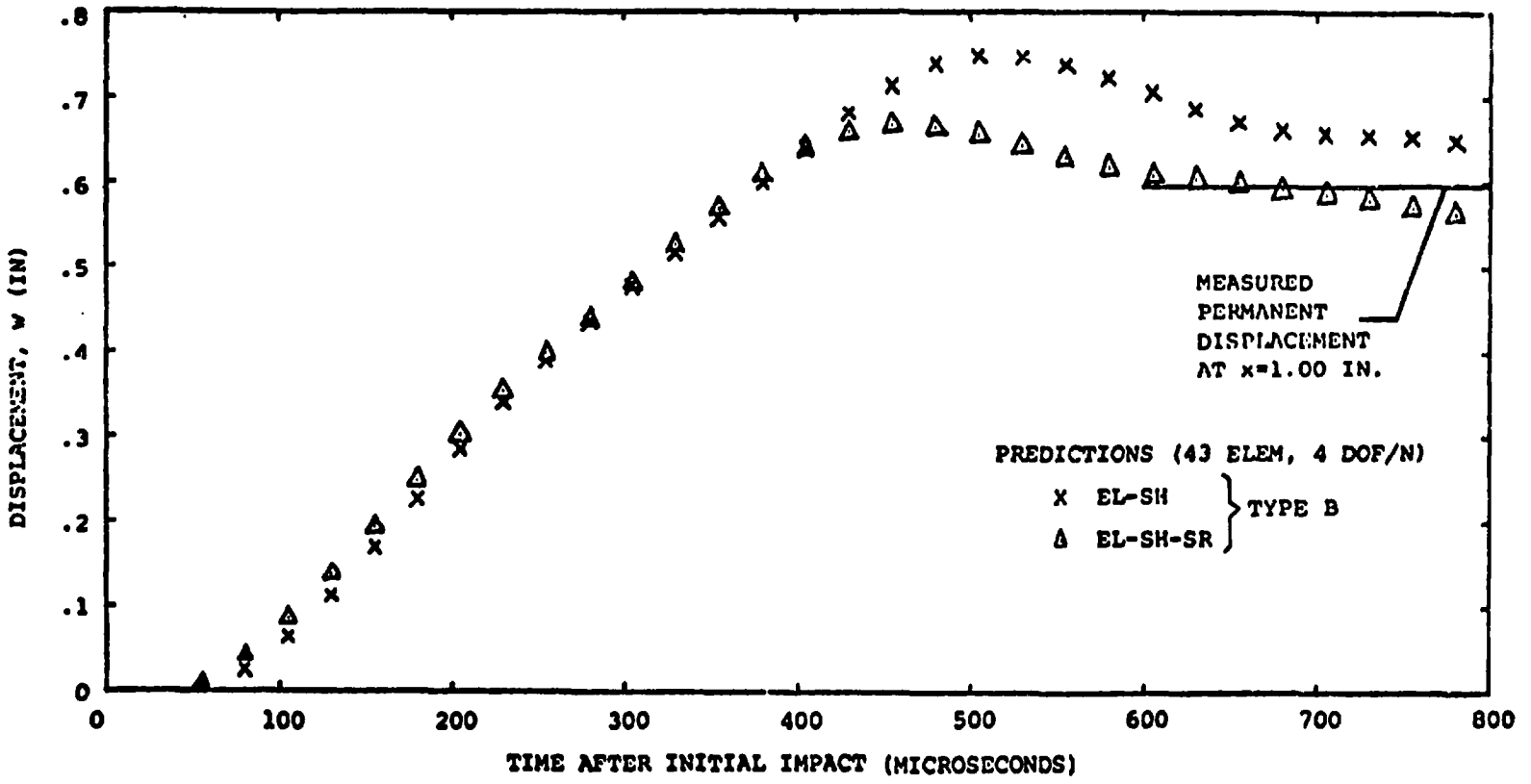

FIG. 20 PREDICTED TRANSIENT AND OBSERVED PERMANENT LATERAL DEFLECTION w AT SPANWISE STATION x=1.0 IN FOR STEEL-SPHERE IMPACTED 6061-T651 ALUMINUM BEAM SPECIMEN CB-18

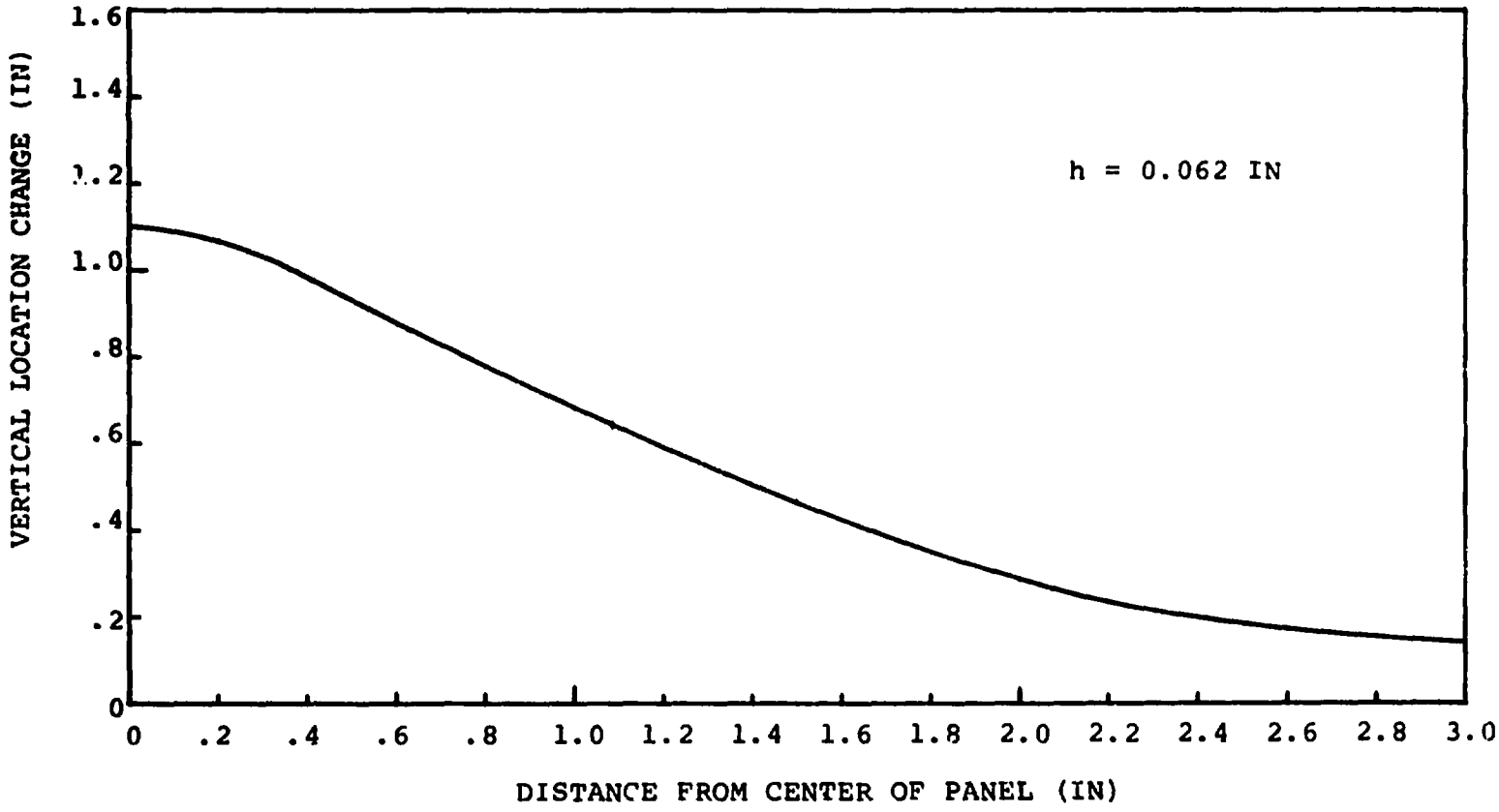

FIG. 21 PERMANENT LATERAL DEFLECTION OF IMPULSIVELY-LOADED SQUARE 6061-T651 ALUMINUM PANEL MODEL CP-2 WITH ALL FOUR SIDES IDEALLY CLAMPED

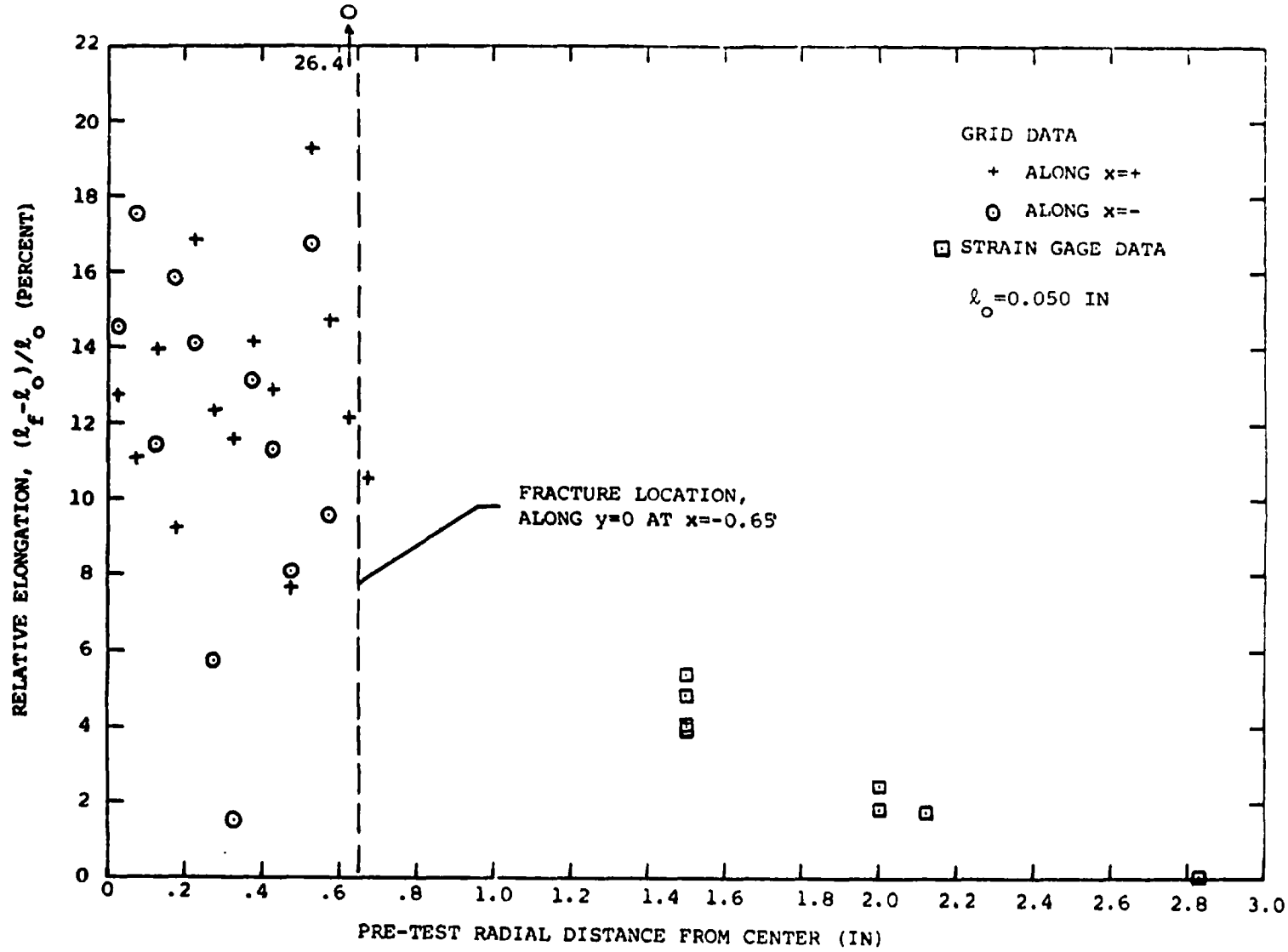

FIG. 22 UPPER SURFACE PERMANENT RELATIVE ELONGATION DATA FOR IMPULSIVELY-LOADED PANEL MODEL CP-2

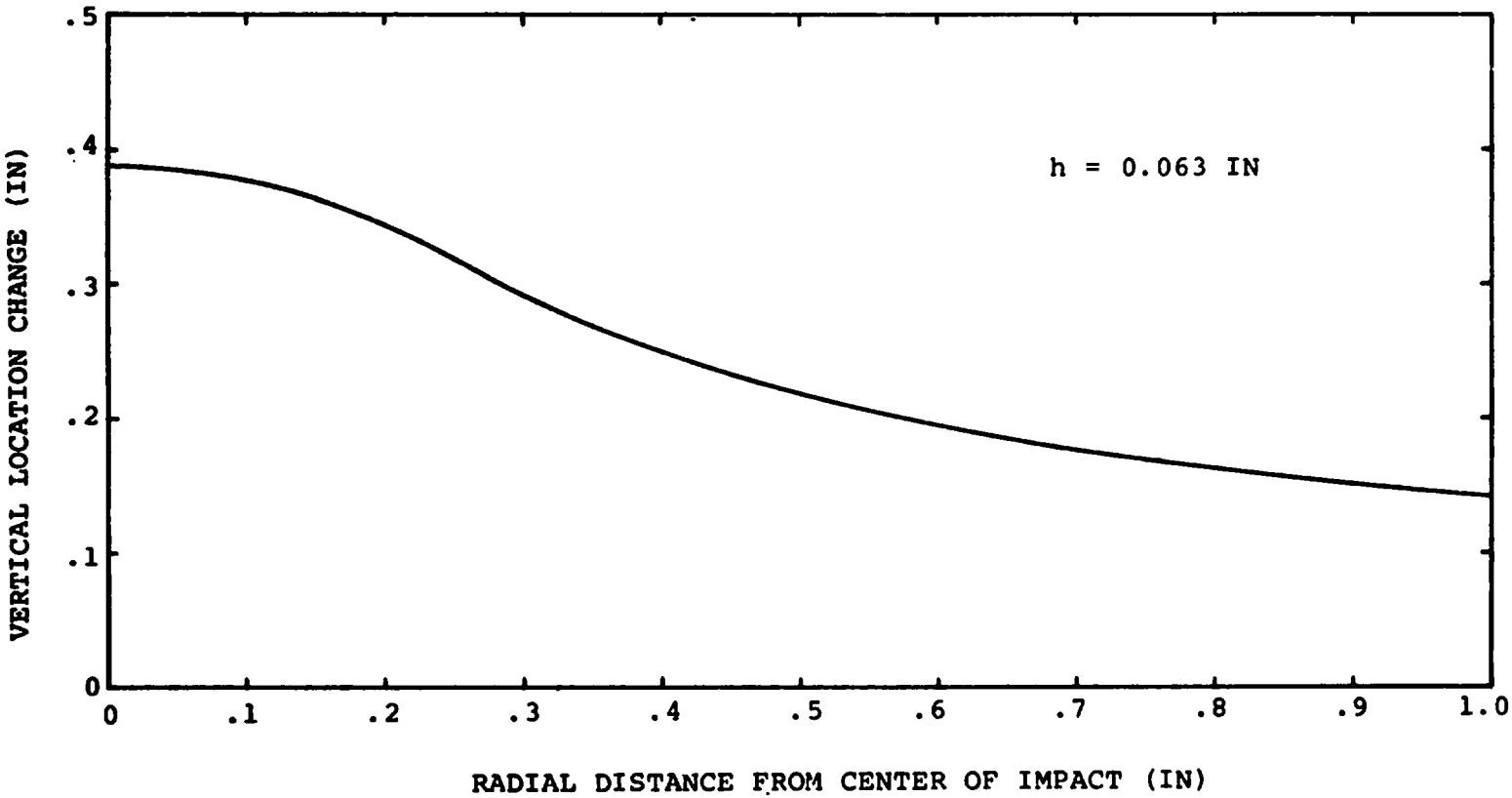

FIG. 23 PERMANENT LATERAL DEFLECTION OF STEEL-SPHERE IMPACTED 6061-T651 ALUMINUM PANEL MODEL CP-8

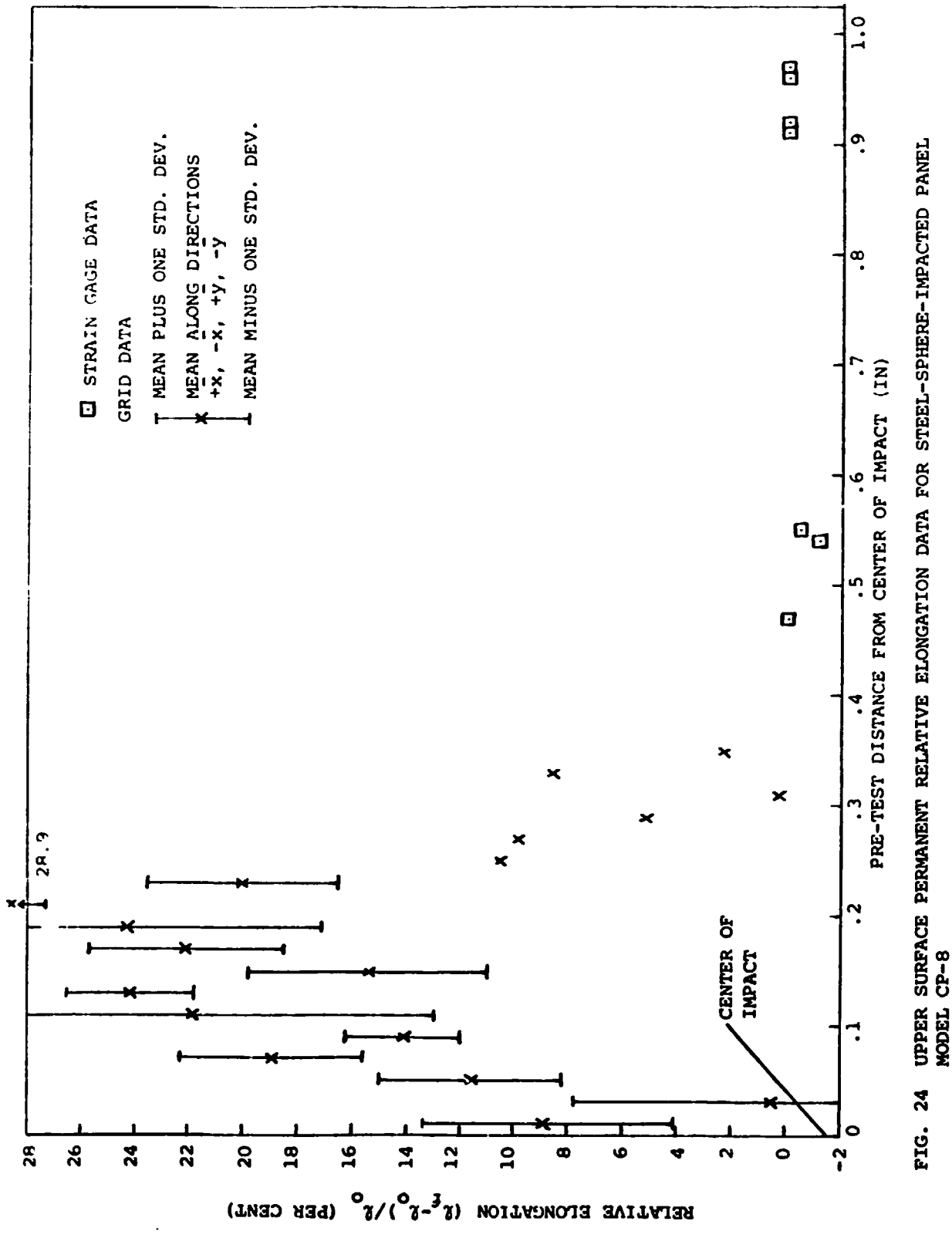

FIG. 24 UPPER SURFACE PERMANENT RELATIVE ELONGATION DATA FOR STEEL-SPHERE-IMPACTED PANEL MODEL CP-8

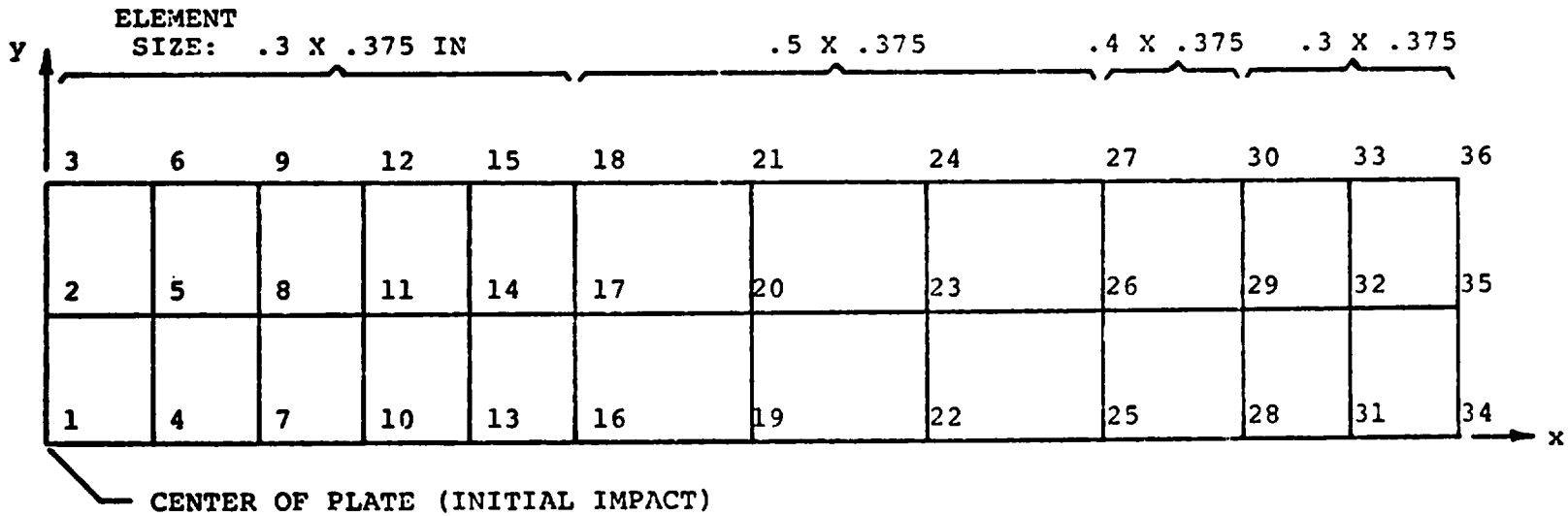

FIG. 25 FINITE ELEMENT ARRAY USED TO REPRESENT ONE QUARTER OF NARROW-PLATE SPECIMEN CB-18

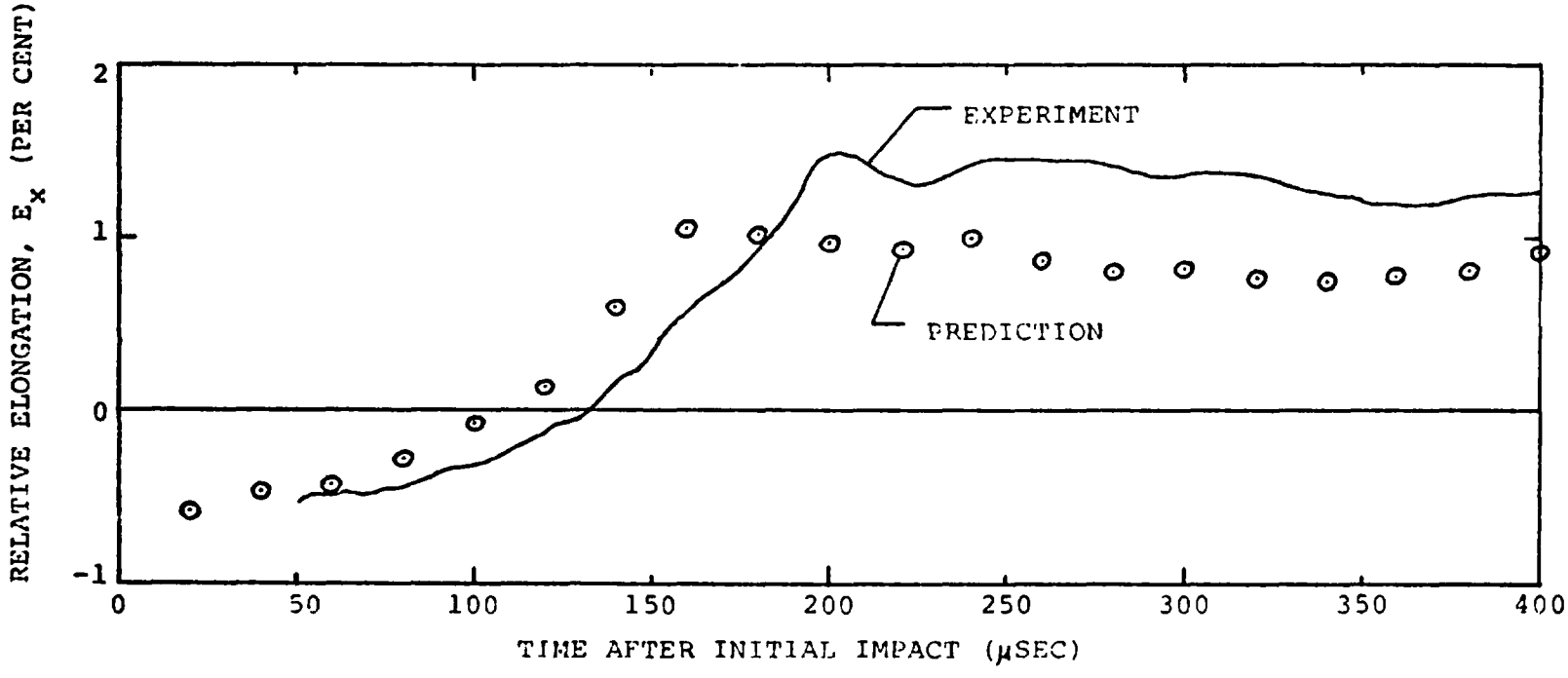

(a) x = 0.6 IN; UPPER SURFACE

FIG. 26 COMPARISON OF PREDICTED AND MEASURED TRANSIENT RELATIVE ELONGATIONS E_x AT VARIOUS SPANWISE STATIONS x ALONG y=0 FOR STEEL-SPHERE-IMPACTED NARROW-PLATE SPECIMEN CB-18

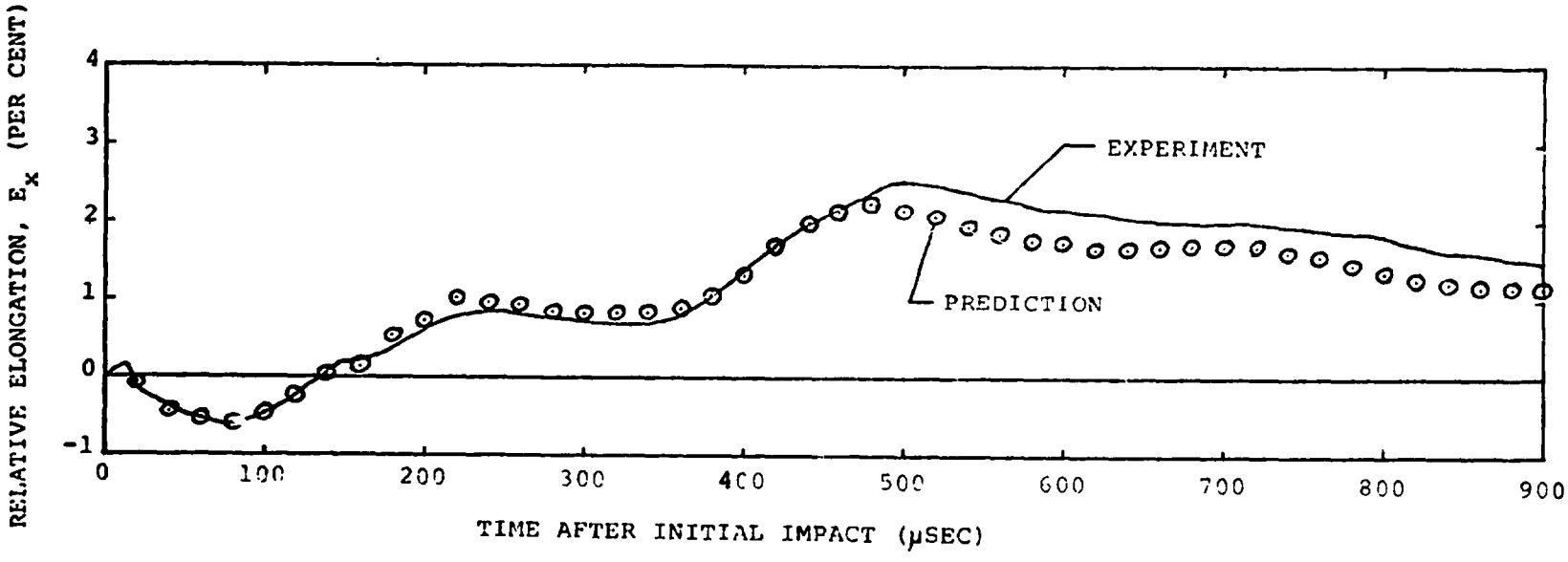

(b) x = 1.2 IN; UPPER SURFACE

FIG. 26 CONCLUDED (NARROW PLATE CB-18)

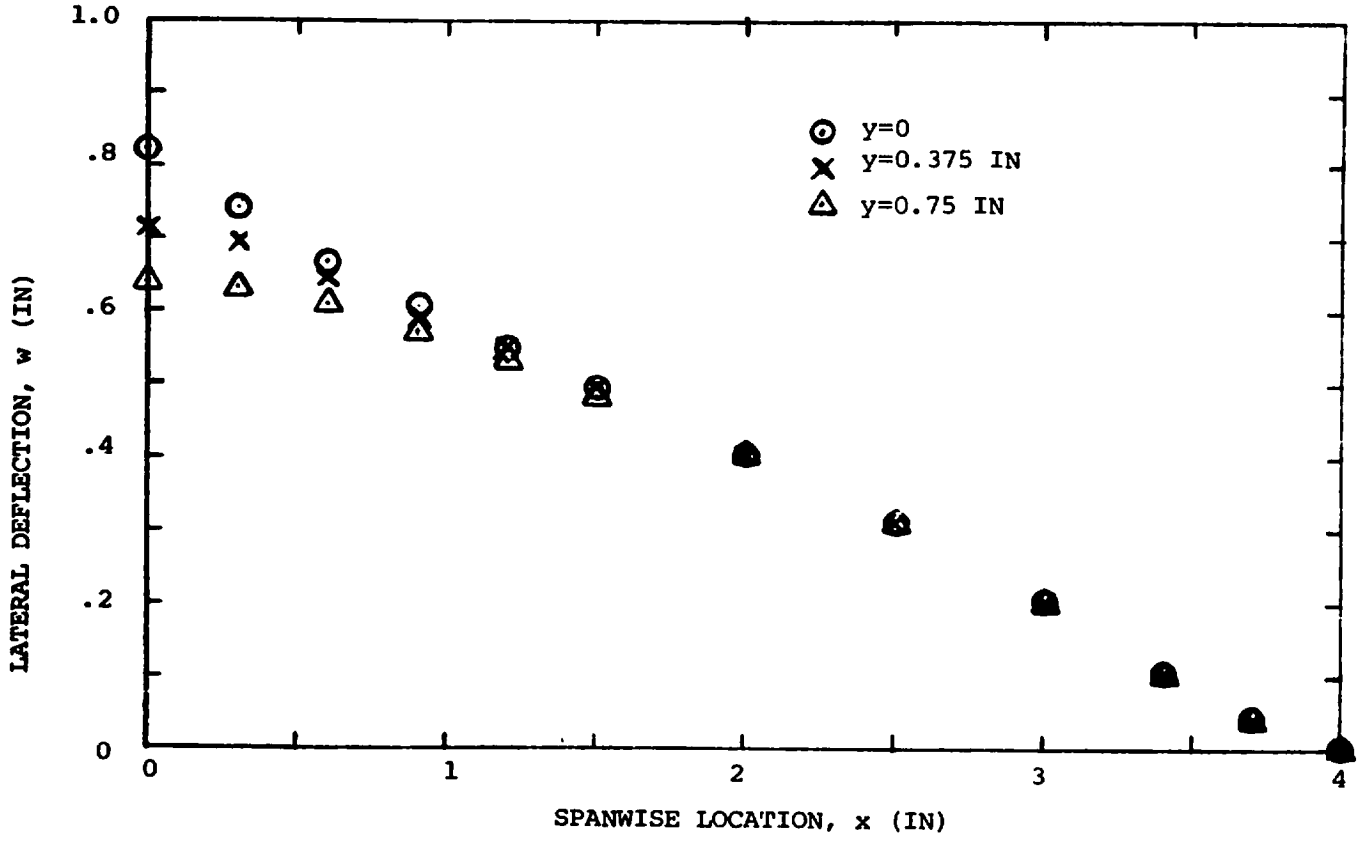

FIG. 27 PREDICTED LATERAL DEFLECTION DISTRIBUTION AT 900 MICROSECONDS AFTER INITIAL IMPACT FOR NARROW-PLATE SPECIMEN CB-18

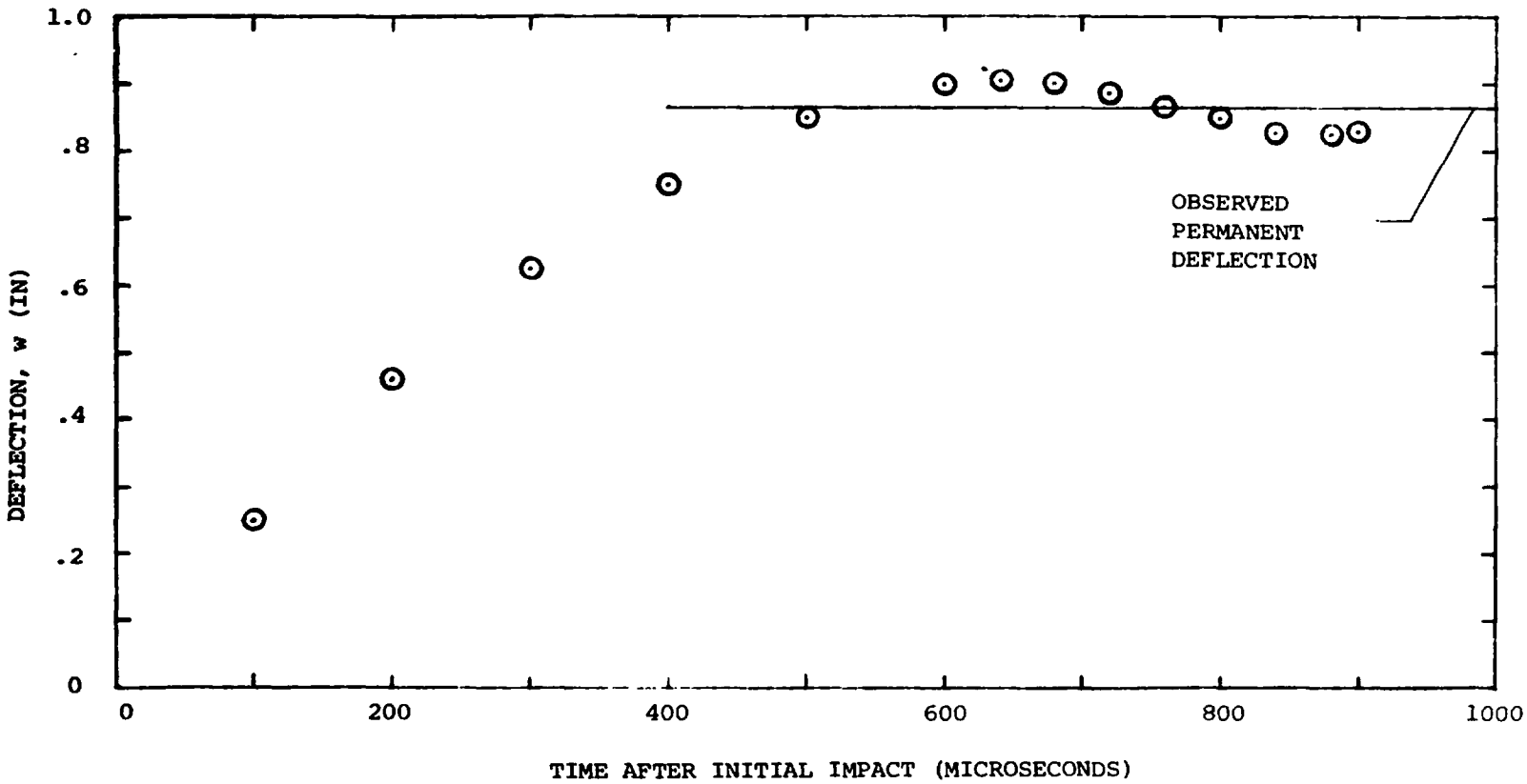

FIG. 28 PREDICTED TRANSIENT AND MEASURED PERMANENT DEFLECTION OF NARROW-PLATE SPECIMEN CB-18 AT PANEL CENTER (x,y)=(0,0)

APPENDIX A

SUMMARY OF THE CAPABILITIES OF MIT-ASRL COMPUTER CODES FOR PREDICTING TWO-DIMENSIONAL LARGE-DEFLECTION ELASTIC-PLASTIC TRANSIENT RESPONSES OF RING STRUCTURES

This description is intended to provide for the reader a convenient tabular summary of the principal features and capabilities of the two-dimensional transient large-deflection elastic-plastic structural response ring codes JET 1 (Ref. 1), JET 2 (Ref. 2), JET 3A-3D (Ref. 3), CIVM-JET 4B (Ref. 4), and JET 5A and CIVM-JET 5B (Ref. 5) developed under NASA NGR 22-009-339.

The JET 1 code of Ref. 1 pertains to single-layer complete, uniform-thickness, initially-circular rings of either temperature-independent or temperature dependent material properties. These rings may be subjected to prescribed: (a) initial velocities, (b) transient mechanical loading, and/or (c) steady nonuniform temperatures. The finite-difference method employed in this code had been shown previously (Ref. 6) to provide reliable predictions for the case of temperature-independent material properties.

The JET 2 code was written in order to extend this finite-difference analysis capability to treat multilayer rings -- cases anticipated to be of future concern. In the interests of efficiency and the minimization of computer storage requirements, temperature-dependent material properties and thermal loading features were omitted from JET 2; if these omitted features should turn out to be needed urgently, they could be added later.

Since the JET 1 and JET 2 codes pertained to initially-circular, complete rings of uniform thickness whereas there was interest also in variable-thickness, arbitrarily curved, partial as well as complete rings, the JET 3 series codes was developed. To accommodate these latter features as well as a variety of types of (1) boundary conditions, (2) elastic-foundation supports, and (3) point elastic supports, the more versatile finite-element analysis procedure was developed and employed. For efficiency and user convenience, four versions of the JET 3 program were developed; each version accommodates both complete rings and partial rings. JET 3A and JET 3B pertain to uniform-thickness, initially-circular rings, and employ, respectively, the central-difference and the Houbolt finite-difference time operator; for certain cases, the latter finite-difference time operator may permit more economic converged transient response predictions than the former. The codes JET 3C and JET 3D are corresponding codes which accommodate variable-thickness, arbitrarily-curved rings.

In most of these codes (JET 1 through JET 3D and JET 5A), the stimuli: (1) initial velocity or impulse conditions and/or (2) transient mechanical loading must be prescribed by the user or analyst. The externally-applied forces experienced by a complete or a partial ring from fragment impact are not provided within these codes. The user must supply his own estimate of the distribution and time histories of these forces. However, in the CIVM-JET 4B and CIVM-JET 5B codes, fragment/ring interaction and response effects are handled internally automatically, for the idealized single-fragment and n-fragment cases provided and discussed in the Appendices of Refs. 4, 5, and 7.

The CIVM-JET 4B code (Ref. 4) was developed from a modified version of the JET 3C code, using the central difference timewise operator. The CIVM (collision imparted velocity method) handles a fragment-structure impact as a series of quasi-static momentum transfers between the attacking fragment and the local-impact-affected portion of the impacted structure. The solution proceeds as though a series of impulses has been applied to the impacted region of the structure. This code provides strain output at each Gaussian station, nodal location, and designated additional points for user convenience, and calculates the reaction forces at each constrained degree of freedom. Another feature of this code is the ability to accommodate branches which are used as additional structural supports. These branches can have material properties either the same or different from those present in the main structure.

The JET 5A and CIVM-JET 5B codes (Ref. 5) were written in order to extend the capabilities of the JET 3D and CIVM-JET 4B codes to multilayer structures which are assumed to be hard-bonded and to deform in the Bernoulli-Euler fashion. Both codes contain the Houbolt timewise operator and all the additional strain and reaction force output and structural support capabilities utilized in the CIVM-JET 4B code.

In convenient tabular form, the principal features and capabilities of the codes JET 1, JET 2, JET 3A-D, CIVM-JET 4B, JET 5A, and CIVM-JET 5B are given in the following:

REFERENCES

1. McCallum, R.B., Leech, J.W. and Witmer, E.A., "Progress in the Analysis of Jet Engine Burst-Rotor Containment Devices", ASRL TR 154-1, Aeroelastic and Structures Research Laboratory, Massachusetts Institute of Technology, August 1969. (Available as NASA CR-107900.)

2. McCallum, R.B., Leech, J.W. and Witmer, E.A., "On the Interaction Forces and Responses of Structural Rings Subjected to Fragment Impact", ASRL TR 154-2, Aeroelastic and Structures Research Laboratory, Massachusetts Institute of Technology, September 1970. (Available as NASA CR-72801.)

3. Wu, R.W.-H. and Witmer, E.A., "Computer Program - JET 3 - to Calculate the Large Elastic-Plastic Dynamically-Induced Deformations of Free and Restrained, Partial and/or Complete Structural Rings", ASRL TR 154-7, Aeroelastic and Structures Research Laboratory, Massachusetts Institute of Technology, August 1972. (Available as NASA CR-120993.)

4. Stagliano, T.R., Spilker, R.L. and Witmer, E.A., "User's Guide to Computer Program CIVM-JET 4B to Calculate the Transient Structural Responses of Partial and/or Complete Structural Rings to Engine Rotor Fragment Impact", MIT ASRL TR 154-9, March 1976. (Available as NASA CR-CR-134907.)

5. Wu, R.W.-H., Stagliano, T.R., Witmer, E.A. and Spilker, R.L., "User's Guide to Computer Programs JET 5A and CIVM-JET 5B to Calculate the Large Elastic-Plastic Dynamically-Induced Deformations of Multilayer Partial and/or Complete Structural Rings", MIT ASRL TR 154-10, February 1977.

6. Balmer, H.A. and Witmer, E.A., "Theoretical-Experimental Correlation of Large Dynamic and Permanent Deformations of Impulsively-Loaded Simple Structures", Massachusetts Institute of Technology, AFFDL-TDR-64-108, July 1964.

7. Collins, T.P. and Witmer, E.A., "Application of the Collision-Imparted Velocity Method for Analyzing the Responses of Containment and Deflector Structures to Engine Rotor Fragment Impact", ASRL TR 154-8, MIT, August 1973. (Available as NASA CR-134494.)

Feature	JET 1 (Ref.1)	JET 2 (Ref.2)	JET 3A (Ref.3)	JET 3B (Ref.3)	JET 3C (Ref.3)	JET 3D (Ref.3)	CIVM-JET 4B (Ref.4)	JET 5A (Ref.5)	CIVM-JET 5B (Ref.5)
Type of Spatial Analysis Formulation									
Finite Difference	x	x	-	-	-	-	-	-	-
Finite Element	-	-	x	x	x	x	x	x	x
Type of Finite-Difference Time Operator									
Central Difference	x	x	x	-	x	-	x	-	-
Houbolt (Backward Difference)	-	-	-	x	-	x	-	x	x
Ring Geometry									
Complete Ring	x	x	x	x	x	x	x	x	x
Partial Ring	-	-	x	x	x	x	x	x	x
Initial Configuration									
Circular	x	x	x	x	x	x	x	x	x
Arb. Curved	-	-	-	-	x	x	x	x	x
Constant Thickness	x	x	x	x	x	x	x	x	x
Variable Thickness	-	-	-	-	x	x	x	x	x
Single Layer	x	x	x	x	x	x	x	x	x
Multilayer Hard-Bonded (1 to 3 layers)	-	x	-	-	-	-	-	x	x
Boundary Conditions									
Ideally Clamped	-	-	x	x	x	x	x	x	x
Hinged Fixed	-	-	x	x	x	x	x	x	x
Symmetry	-	-	x	x	x	x	x	x	x
Free	-	-	x	x	x	x	-	x	-
Other Support Conditions									
Distributed Elastic Foundation	-	-	x	x	x	x	x	x	x
Point Elastic Springs	-	-	-	x	x	x	x	x	x
Structural Branch	-	-	-	-	-	-	x	x	x

Feature	JET 1	JET 2	JET 3A	JET 3B	JET 3C	JET 3D	CIVM-JET 4B	JET 5A	CIVM-JET 5B
Material									
Single Material	x	-	x	x	x	x	x	x	x
Different for Each Layer	-	x	-	-	-	-	-	x	x
Homogeneous	x	x	x	x	x	x	x	x	x
Initially Isotropic	x	x	x	x	x	x	x	x	x
Temperature Independent	x	x	x	x	x	x	x	x	x
Temperature Dependent	x	-	-	-	-	-	-	-	-
EL	x	x	x	x	x	x	x	x	x
EL-PP	x	x	x	x	x	x	x	x	x
EL-LSH	x	x	x	x	x	x	x	x	x
EL-SH	x	x	x	x	x	x	x	x	x
EL-SH-SR	x	x	x	x	x	x	x	x	x
Stimulii									
Initial Velocity									
Arbitrary	x	x	x	x	x	x	-	x	-
Half-Sine over each of Selected Regions	x	x	x	x	x	x	-	x	-
Mechanical Loading									
Arbitrary Spatial Distribution with Arb. Time History	-	x	x	x	x	x	-	x	-
Half-Sine over each of Selected Regions	x	x	x	x	x	x	-	x	-
Triangular Time History	x	x	x	x	x	x	-	x	-
Arbitrary Time History	-	x	x	x	x	x	-	x	-
Thermal Loads (Temp. Distribution)									
Distribution Thru Thickness	x	-	-	-	-	-	-	-	-
Time-Independent Prescribed Circumferential Distribution	x	-	-	-	-	-	-	-	-
Impacting Fragments									
Single	-	-	-	-	-	-	x	-	x
Multiple	-	-	-	-	-	-	x	-	x
Friction	-	-	-	-	-	-	x	-	x

Feature	JET 1	JET 2	JET 3A	JET 3B	JET 3C	JET 3D	CIVM-JET 4B	JET 5A	CIVM-JET 5B
Deflections: Bernoulli-Euler Type Only									
Small	x	x	x	x	x	x	x	x	x
Arbitrarily Large	x	x	x	x	x	x	x	x	x
OUTPUT INFORMATION									
At Selected Times									
Energy/Work Type and Amount	x	x	x	x	x	x	x	x	x
Nodal Station Data									
Locations Y,Z	x	x	x	x	x	x	x	x	x
Displacements	-	-	x	x	x	x	x	x	x
Moment Resultant	x	x	x	x	x	x	x	x	x
Circum. Force Resultant	x	x	x	x	x	x	x	x	x
Circumferential Strains									
Inner Surface	x	x	x	x	x	x	x	x	x
Outer Surface	x	x	x	x	x	x	x	x	x
Location where Prescribed Value is Exceeded	-	x	x	x	x	x	-	-	-
Strain at Gaussian Stations	-	-	-	-	-	-	x	x	x
Strain at Additional Location	-	-	-	-	-	-	x	x	x
Support Reaction Forces	-	-	-	-	-	-	x	x	x
At Certain Other Times									
Time of First Yielding	x	x	-	-	-	-	-	-	-
Time when Strain First Exceeds a Prescribed Value	-	x	x	x	x	x	-	-	-
Time, Location, and Value of Largest Strain Reached During Run	-	-	x	x	x	x	x (For Each Substructure)	x	x
CAPACITY INFORMATION									
Maximum No. of Finite-Difference Stations[a]	100	100	-	-	-	-	-	-	-
Maximum No. of Finite Elements[a]	-	-	50	50	50	50	50	50	50

[a] These limits can be circumvented by altering the dimensions of appropriate program variables (see each source reference).

APPENDIX B

PUBLICATIONS AND TRANSIENT STRUCTURAL RESPONSE COMPUTER CODES BY THE MIT-ASRL ON NASA-SPONSORED FRAGMENT CONTAINMENT/DEFLECTION RESEARCH

1. McCallum, R.B., Leech, J.W. and Witmer, E.A., "Progress in the Analysis of Jet Engine Burst-Rotor Containment Devices", ASRL TR 154-1, Aeroelastic and Structures Research Laboratory, Massachusetts Institute of Technology, August 1969. (Available as NASA CR-107900.)

2. McCallum, R.B., "Simplified Analysis of Trifragment Rotor Disk Interaction with a Containment Ring", AIAA Journal of Aircraft, Vol. 7, No. 3, May-June 1970, pp. 283-285.

3. McCallum, R.B., Leech, J.W. and Witmer, E.A., "On the Interaction Forces and Responses of Structural Rings Subjected to Fragment Impact", ASRL TR 154-2, Aeroelastic and Structures Research Laboratory, Massachusetts Institute of Technology, Sept. 1970. (Available as NASA CR-72801.)

4. Wu, R.W.-H. and Witmer, E.A., "Finite Element Analysis of Large Elastic-Plastic Transient Deformations of Simple Structures", AIAA Journal Vol. 9, No. 9, Sept. 1971, pp. 1719-1724.

5. Leech, J.W., Witmer, E.A., and Yeghiayan, R.P., "Dimensional Analysis Considerations in the Engine Rotor Fragment Containment/Deflection Problem", ASRL TR 154-3, Aeroelastic and Structures Research Laboratory, Massachusetts Institute of Technology, December 1971. (Available as NASA CR-120841.)

6. Wu, R.W.-H. and Witmer, E.A., "Finite-Element Analysis of Large Transient Elastic-Plastic Deformations of Simple Structures, with Application to the Engine Rotor Fragment Containment/Deflection Problem", ASRL TR 154-4, Aeroelastic and Structures Research Laboratory, Massachusetts Institute of Technology, January 1972. (Available as NASA CR-120886.)

7. Zirin, R.M. and Witmer, E.A., "Examination of the Collision Force Method for Analyzing the Responses of Simple Containment/Deflection Structures to Impact by One Engine Rotor Blade Fragment", ASRL TR 154-6, Aeroelastic and Structures Research Laboratory, Massachusetts Institute of Technology, May 1972. (Available as NASA CR-120952.)

8. Wu, R.W.-H. and Witmer, E.A., "Computer Program - JET 3 - to Calculate the Large Elastic-Plastic Dynamically-Induced Deformations of Free and Restrained, Partial and/or Complete Structural Rings", ASRL TR 154-7, Aeroelastic and Structures Research Laboratory, Massachusetts Institute of Technology, August 1972. (Available as NASA CR-120993.)

9. Wu, R.W.-H. and Witmer, E.A., "Approximate Analysis of Containment/Deflection Ring Responses to Engine Rotor Fragment Impact", AIAA Journal of Aircraft, Vol. 10, No. 1, January 1973, pp. 28-37.

10. Wu, R.W.-H. and Witmer, E.A., "Nonlinear Transient Responses of Structures by the Spatial Finite-Element Method", AIAA Journal, Vol. 11, No. 8, August 1973, pp. 1110-1117.

11. Collins, T.P. and Witmer, E.A., "Application of the Collision-Imparted Velocity Method for Analyzing the Responses of Containment and Deflector Structures to Engine Rotor Fragment Impact", MIT ASRL TR 154-8, August 1973. (Available as NASA CR-134494.)

12. Yeghiayan, R.P., Leech, J.W. and Witmer, E.A., "Experimental and Data Analysis Techniques for Deducing Collision-Induced Forces from Photographic Histories of Engine Rotor Fragment Impact/Interaction with a Containment Ring," MIT ASRL TR 154-5, October 1973. (Available as NASA CR-134548.)

13. Witmer, E.A., Merlis, F. and Spilker, R.L., "Experimental Transient and Permanent Deformation Studies of Steel-Sphere-Impacted or Impulsively-Loaded Aluminum Beams with Clamped Ends", MIT ASRL TR 154-11, October 1975. (Available as NASA CR-134922.)

14. Stagliano, T.R., Spilker, R.L. and Witmer, E.A., "User's Guide to Computer Program CIVM-JET 4B to Calculate Large Nonlinear Transient Deformations of Single-Layer Partial and/or Complete Structural Rings to Engine Rotor Fragment Impact", MIT ASRL TR 154-9, March 1976. (Available as NASA CR-134907.)

15. Wu, R.W.-H., Stagliano, T.R., Witmer, E.A. and Spilker, R.L., "User's Guide to Computer Programs JET 5A and CIVM-JET 5B to Calculate the Large Elastic-Plastic Dynamically-Induced Deformations of Multilayer Partial and/or Complete Structural Rings", MIT ASRL TR 154-10, February 1977.

16. Witmer, E.A., Merlis, F., Rodal, J.J.A. and Stagliano, T.R., "Experimental Transient and Permanent Deformation Studies of Steel-Sphere-Impacted or Impulsively-Loaded Aluminum Panels", MIT ASRL TR 154-12, March 1977.

STRUCTURAL RESPONSE COMPUTER CODE STATUS

Code	Capability	Status	Availability
JET 3	2-D Single-Layer Beams and Rings Subjected to Prescribed Transient Loads or Initial Velocity Distributions (No Fragment Impact)	Complete (Ref. 8)	a
CIVM-JET 4B	2-D Single-Layer Beams and Rings Subjected Only to Fragment Impact	Complete (Ref. 14)	b
JET 5A	2-D Multilayer Bernoulli-Euler Beams and Rings Subjected to Prescribed Transient Loads or Initial Velocity Distributions	Complete (Ref. 15)	b
CIVM-JET 5B	2-D Multilayer B-E Beams and Rings Subjected only to Fragment Impact	Complete (Ref. 15)	b
PLATE and CIVM-PLATE	3-D Single Layer Initially-Flat Panels Subjected, Respectively, to (1) Prescribed Transient Loads and/or Initial Velocity Distributions or (2) Fragment Impact Only	In Progress	--

a: Available from COSMIC, Barrow Hall, University of Georgia, Athens, GA. 30601; contact MIT for errata.

b: Available under a copyright licensing agreement from MIT. Contact Prof. E.A. Witmer, Room 41-219, MIT, Cambridge, Mass. 02139.

DISCUSSION

B.L. Koff, GE-Cincinnati

We have conducted tests and managed to collect pieces of blades that were deliberately failed to understand containment ring behavior. It is quite obvious that you don't get a three-lobe shape in the ring, because as soon as the ring starts deforming locally, all of the other blades in the rotor act as a bearing for the ring. This tends to keep the ring round, not three-corner or some other shape, by adding quite a bit of support to the ring. It suggests that there is more to be learned from the tests you are now running on panels, than in oversimplified tests run with a ring that is not supported in a manner similar to the engine. When you start adding other support, you might find that these simplified panel tests, in fact, more nearly duplicate what actually happens, than an oversimplified test with rotor burst fragments.

E.A. Witmer, MIT-ASRL

I think it would be very useful in this whole program, if we could have people like you, who could suggest to us proper models to use for supported structures, so that we simulate things in the right way. It's an excellent idea.

As I understand your described tests, you released 1 or 2 blade portions from a rotating fully-bladed rotor to impact a containment ring. Similar tests done at the NAPTC show behavior very similar to what you describe; the initial impact causes the ring to deform and then it comes in contact with the blades still attached to the spinning rotor. These blades also deform but do "support" the ring and tend to restrain it from deforming as severely as it would if a "free ring" were impacted only by the initial attacking fragments.

A. Weaver, P&W

As I understand this model, it does a fairly representative job of modelling deflections in simple structures, whether they are panels or rings. However, it doesn't get at the meat of the containment problem as I see it, which is failure. I don't always care about deflections, but I do care when and where the ring is going to fail, and how to model that. The 2-D analysis completely ignored the localized effects going on at the center of impact, which I believe are very important.

E.A. Witmer, MIT-ASRL

You're perfectly correct, there are 3-D effects present where failure initiates in the cited beam experiments, and 2-D is clearly an idealization. It's a convenient scheme to us to obtain some crude estimates but it certainly doesn't address the real problem. The 3-D problem is the important one. For the beams and rings discussed here, the structural response behavior is of the 2-D type essentially everywhere on the (narrow) rings and also everywhere on the steel-sphere-impacted beam specimens except near the "impact point" itself where 3-D effects are very prominent. Here at threshold rupture, a multiaxial

strain state involving very large strains exists. For such regions, the analysis must accommodate large strain plasticity effects and an appropriate "failure strain" or similar criterion. This is a matter that is receiving much attention now by various groups.

D. Oplinger, Army-AMMRC

Is it realistic to assume that you're going to get a structural problem rather than a penetration problem? Some of the velocities I saw were fairly low; they were a couple hundred feet per second, but when you get up to a thousand feet per second, you've got to treat the penetration problem first and then you can treat it as a structural response problem.

E.A. Witmer, MIT-ASRL

As I understood the fragment velocities cited, they represent the fragment tip and/or the CG velocities; not the velocity component perpendicular to the impacted surface at impact. For rotors with typical small clearance, the typical impact angle is very shallow -- somewhere in the vicinity of 20-25 degrees. Hence, for many cases, the typical normal-to-the-surface velocity component at impact might range up to perhaps about 420 fps. Depending upon the material properties of the structure being impacted, the subsequent behavior could involve "penetration" followed by structural response or could involve principally only structural response. For most of the containment structure materials being considered, I believe that the latter is the more prevalent case.

D. Oplinger, Army-AMMRC

I am not familiar with blade materials but what little I know would lead me to believe that it would be unusual to get such large curling as you were showing. Is that typical of common blade materials, that they can bend over like that without snapping into small pieces?

E.A. Witmer, MIT-ASRL

For the small T58 turbine rotor used in many of the NAPTC tests, this was the observed behavior. However, for the rotors of the newer larger engines, I will ask Mr. Koff of GE to respond -- he can give a better answer.

B.L. Koff, GE-Cincinnati

Some of the blades are high aspect ratio turbine blades, and are more typical of aft end turbine stages. The first stage of the HP has blades of low aspect ratio and the first stage of an air-cooled turbine consists of a hollow structure which usually fragments into many pieces upon impact. Titanium fan blades don't curl very much but break up into pieces.

S. Sattar, P&W

I want to remark on the basic philosophy or approach to fragment containment design. Would it make more sense for us to step back and ask ourselves that if you go through this analysis and you have to determine when these computer programs will predict penetration, you would have to calibrate them against tests? Might it not be easier to take a simpler approach to predict

whether the fragment will be contained or not? It is a case of strength of materials or solid mechanics approach, calibrated against spin-pit or specimen tests versus these codes to predict the deflections and strains, and then finding out at what strain value will the penetration finally take place -- which you will calibrate anyway, against some tests. I would like a comment on that.

E.A. Witmer, MIT-ASRL

Your point is, a valid one, however, I think that if one can afford to run experiments on every kind of configuration, material, and so forth, to obtain the data you seek, that's one way of proceeding. There is some hope that one need not go that far, but instead one can rely upon more basic material property information and methods of structural dynamic analysis (at least for simple cases) and have a reasonable prospect of predicting analytically when these containment-structure failures should occur. I believe that the 3-D structural response studies in progress represent a useful step in that direction.

Now, one can immediately dream up a new case which is too complicated for any available analysis to handle properly. In such cases one would have to appeal to selected experiments; it seems to me any good organization would always do that.

J.W. Leech, ERDA

Would you comment on why an aluminum alloy was used for the beam model, the panel models, and the containment ring which was subjected to single-blade impact.

E.A. Witmer, MIT-ASRL

We used 6061-T6 and 6061-T651 aluminum for these specimens for fabrication convenience and because their stress-strain properties are well known; very little strain hardening is present. We approximated these properties by piecewise linear segments and used them (via the mechanical sublayer model) in the transient response calculations.

Incidentally, the NAPTC had static stress-strain tests conducted on the 4130 cast steel used in their containment ring tests. As perhaps you noticed, we did not show any comparisons between our calculations and the experiment for NAPTC Test 201 (T58 tri-hub burst against the steel containment ring) because we have not concluded that work. You can see immediately that the idealization that we used for the fragment, will give us no hope whatever of predicting in detail the transient response. The hope is that a realistic selection of the idealized (rigid circular) fragment may enable us to predict the peak response reasonably well, but the actual physical situation is just so much different from the idealized model that the fine transient response details actually present can not be reproduced by this model. But that's really expecting too much of that simple model. Of course, the model can be refined. One can devise a more complicated fragment model -- one can put in the various curling blades (attached to the disk segment) and let them go ahead and curl and follow them; a tremendous amount of bookkeeping would be involved.

Hence, we elected to try to see the potential of this simple rigid-circular-fragment idealization. Also, one could modify this simple circular fragment to permit deformations approximating roughly the behavior of the blade/disk fragment itself to achieve a still simple, but better simulation of the actual attacking fragment.